Synthesis and *in silico* studies of pyrazoline containing quinoline derivatives as anti-HIV agents

Thesis submitted to the Central University of Punjab

For the award of

Master of Pharmacy (Medicinal Chemistry)

In

Department of Pharmaceutical Sciences and Natural Products

By

Diksha Choudhary

(Reg. No.: 16mpharm11)

Supervisor

Dr. Pradeep Kumar

Department of Pharmaceutical Sciences and Natural Products

School of Basic and Applied Sciences

Central University of Punjab, Bathinda

June, 2018

DECLARATION

I declare that the thesis entitled **"Synthesis and *in silico* studies of pyrazoline containing quinoline derivatives as anti-HIV agents"** has been prepared by me under the guidance of Dr. Pradeep Kumar, Assistant Professor, Department of Pharmaceutical Sciences and Natural Products, School of Basic and Applied Sciences, Central University of Punjab, Bathinda. No part of this thesis has formed the basis for the award of any degree or fellowship previously.

(Diksha Choudhary)

Department of Pharmaceutical Sciences and Natural Products,

School of Basic and Applied Sciences,

Central University of Punjab,

Bathinda – 151001

Date:

CERTIFICATE

I certify that Diksha Choudhary has prepared her thesis entitled **"Synthesis and *in silico* studies of pyrazoline containing quinoline derivatives as anti-HIV agents"** for the award of M. Pharmacy (Medicinal Chemistry) degree at the Central University of Punjab, under my guidance. She has carried out this work at the Department of Pharmaceutical Sciences and Natural Products, School of Basic and Applied Sciences, Central University of Punjab, Bathinda.

Dr. Pradeep Kumar

Assistant Professor

Department of Pharmaceutical Sciences and Natural Products,

School of Basic and Applied Sciences,

Central University of Punjab,

Bathinda- 151001

Date:

ABSTRACT

Synthesis and *in silico* studies of pyrazoline containing quinoline derivatives as anti-HIV agents

Name of student	:	Diksha Choudhary
Registration Number	:	16mpharm11
Degree for which submitted	:	M. Pharmacy (Medicinal Chemistry)
Department	:	Pharmaceutical Sciences and Natural Products
School of Studies	:	Basic and Applied Sciences

Quinoline moiety is an important scaffold in the field of drug discovery and drug development with wide range of pharmacological activities. Its derivatives are potent inhibitors for reverse transcriptase which is responsible for the conversion of single strand viral RNA into double strand viral DNA. In the present study, we have designed and synthesized Pyrazoline containing quinoline derivatives as anti-HIV agents. Six compounds were synthesized and characterized by ^{1}H and ^{13}C NMR and Mass spectrophotometry. The synthesized compounds were also docked on HIV binding site (PDB: 4I2P) and most of these showed good binding interactions with the active domain of the receptor. Our synthesized compounds **DC1** and **DC6** showed better binding interactions as compared to standard inhibitor **Elvitegravir.**

Diksha Choudhary Dr. Pradeep Kumar

Acknowledgement

This thesis is the end of my journey in obtaining my M. Pharmacy degree. This thesis has been kept on track and been seen through to the completion with the support, help and encouragement of numerous people including my well-wishers, my family, my friends and colleagues. At the end of my thesis, I would like to thank all those people who made this thesis possible and an unforgettable experience for me.

I would first like to thank my thesis supervisor **Dr. Pradeep Kumar,** Assistant Professor, Department of Pharmaceutical Sciences and Natural Products for his guidance, valuable advice, support and encouragement throughout my research work. The door to his office was always open whenever I ran into a trouble spot or had a question about my research or writing. He consistently allowed this to be my own work, but steered me in the right the direction whenever he thought I needed it. It was a pleasure working with him.

I would like to thank **Dr. Raj Kumar, Associate Professor, Dr. Vinod Kumar, Assistant Professor, Dr. Vikas Jaitak and Dr. Venkata Rao Kaki, Assistant Professor,** Department of Pharmaceutical Sciences and Natural Products for their guidance and support through all the years.

I wish to express my warm and sincere thanks to **Prof. (Dr.) R.K. Kohli, Vice Chancellor and Prof. (Dr.) P. Ramarao, Dean Academic Affairs, Central University of Punjab, Bathinda** for providing me the necessary facilities for carrying out the research.

I am highly thankful to my senior **Ashishranjan Dwivedi** and **Bhupinder Mittal and Ramit Singla and Amit Kumar, Vijay Kumar** for their kind suggestion and support. I would like to thank all my batch mates **Amandeep Thakur, Arvind, Partha Pratim Das, Haris and Sahil, Sonia** for helping and supporting me throughout my work.

I would like to extend my thanks to **Mr. Rajesh Tiwari,** Junior Technical Assistant for their time to time help in the lab and my sincere thanks to my fellows who helped me directly or indirectly.
Diksha Choudhary

TABLE OF CONTENTS

LIST OF TABLES

List of Figures

LIST OF ABBREVIATION

S. No.	Full Form	Abbreviation
1.	2-Dimensional	2-D
2.	3-Dimensional	3-D
3.	Human immune virus	HIV
4.	Hertz	Hz
5.	Coupling constant	J
6.	Multiplet	M
7.	Fourier transform infrared	FT-IR
8.	Doublet	D
9.	Dichloromethane	DCM
10.	Millilitre	mL
11.	Deoxyribonucleic acid	DNA
12.	Food and Drug Administration	FDA
13.	Millimole	mmoL
14.	Melting point	mp
15.	Nuclear magnetic resonance	NMR
16.	Structure activity relationship	SAR
17.	Protein data bank	PDB
18.	Round bottom flask	RBF
19.	Ribonucleic acid	RNA
20.	Room temperature	RT
21.	Singlet	S
22.	Triplet	T
23.	Thin layer chromatography	TLC
24.	Ultraviolet	U.V

25.	Extra precision	XP
26.	Acquired immunodeficiency syndrome	AIDS
27.	Cell mediated immunity	CMI
28.	Dendritic cells	DCs
29.	Antiretroviral therapy	ART
30.	Union Ministry of Health & Family Welfare	MH&FW
31.	Glycoprotein	Gp
32.	Proteins	P
33.	Nucleoside reverse transcriptase inhibitors	NRTIs
34.	Non-nucleoside reverse transcriptase inhibitors	NNRTIs
35.	Protease inhibitors	PIs
36.	Fusion inhibitors	FIs
37.	Highly active antiretroviral therapy	HAART
38.	Stuart melting point	SMP
39.	Dimethyl sulfoxide	DMSO

CHAPTER 1

INTRODUCTION

1.0 Introduction

HIV is human immune-deficient virus which is a retrovirus. The first cases of acquired immunodeficiency syndrome (AIDS) was reported in the United States in the spring of 1981(Rhodes, Chang, Regan, Singer, & Triant, 2017). These are the drugs which are used for prolonging and improving the quality of life and improving the complications of AIDS (acquired immunodeficiency syndrome), but not cure the infection. (Male, Brostoff, & Roth, 2007). Generally, the white cells and antibodies that attack virus and bacteria are produced in immune system. T-cell lymphocytes are known as infection fighting cell. Years to years after a people get infected by HIV; the virus starts destroy T-cell lymphocytes. After that it starts defecting the immune system to defend the body against disease(Male et al., 2007). Over the past 30 years, a number of virus specific targets have been identified and drugs are also developed for the treatment of HIV. Now we have drugs which effectively suppress HIV replication and restore CMI (cell mediated immunity) for variable periods of time.

The two established targets for anti-HIV attack are:

(A). HIV reverse transcriptase: which transcripts HIV-RNA into proviral DNA.

(B). HIV protease: which cleaves the large virus directed polyprotein into functional viral proteins.

The first anti-HIV or anti-retrovirus drug Zidovudine was made and available for use in 1987. Recently some few new targets drugs have also become available for use in patients who have failed several regimens employing the 3 major groups of drugs, and have viral multiplication despite optimized background therapy. The main aim of use of anti-HIV therapy is to cause maximal suppression of viral replication for the maximal period of time that is possible. (Jonathan Brostoff, et al., 1998).

There are 2 type of HIV:

a) HIV-1.
b) HIV-2.

Both are responsible for acquired immune deficiency syndrome (AIDS).

a) HIV-1: Most AIDS infection are caused due to HIV-1 type strains. Infection with HIV type 1 (HIV-1) typically occurs across mucosal surfaces or by direct inoculation. The virus first encounters dendritic cells (DCs), which subsequently facilitate spread of HIV-1 to CD4+ T lymphocytes. DC-SIGN, an HIV-specific DC receptor, binds HIV-1 at its gp-120 domain without requiring direct infection of the cell, and transports HIV-1 to lymphoid tissue (Alam, Whyte-Allman, Omeragic, & Bendayan, 2016). Infected and uninfected cells traffic to regional lymph nodes, where HIV-1 resides and replicates for days to weeks(Chesna & Fellner, 2017). DCs act as potent antigen-presenting cells, priming naive T cells and enabling rapid infection of T cells (Nguyen et al., 2017).

HIV-1 entry into host cells requires docking and binding at 2 separate sites: the CD4+ T cell receptor and a 7-transdomain chemokine coreceptor. Genetic mutations in the CCR5 coreceptor have afforded relative protection from infection with macrophage-tropic strains of HIV-1 in both homozygous and heterozygous individuals; highly exposed and persistently seronegative patients have been shown to carry the CCR5δ32 genotype more frequently (Ikuma et al., 2016). This mutation has been associated with slower disease progression and is more prevalent among patients with long-term nonprogressive disease than among those with progressive disease. (Kassutto & Rosenberg, 2004)

b) HIV-2: HIV-2 is an important cause of disease in West Africa, where it is endemic. HIV-2 infection has also been described in locales with cultural and socioeconomic ties to West Africa, including the United States. It is an important consideration in patients with an AIDS-like illness or among persons with epidemiologic risk factors for infection. Epidemiologic risk factors are similar to HIV-1 infection and include a past history of blood transfusion or having a sex partner or needle-sharing partner with HIV-2 infection or perinatal transmission from an HIV-2-infected mother (Matheron et al., 2018)

1.1. Current status of HIV

There were approximately 36.7 million people worldwide living with HIV/AIDS at the end of 2015. Of these, 1.8 million were children (<15 years old). An

estimated 2.1 million individuals worldwide became newly infected with HIV in 2015. This includes 150,000 children (<15 years). Most of these children live in sub-Saharan Africa and were infected by their HIV-positive mothers during pregnancy, childbirth or breastfeeding. Currently only 60% of people with HIV know their status (Barrientos, Gomez, & Cardenas, 2017). The remaining 40% (over 14 million people) still need to access HIV testing services. In June 2016, 18.2 million people living with HIV were accessing antiretroviral therapy (ART) globally, up from 15.8 million in June 2015, 7.5 million in 2010, and less than one million in 2000. The vast majority of people living with HIV are in low- and middle-income countries. Sub-Saharan Africa is the most affected region, with an estimated 25.6 million people living with HIV in 2015 (Swain, Das, Jha, & Sharnngadharan, 2017). About 66% of new HIV infections in 2015 occurred in sub-Saharan Africa. An estimated 35 million people have died from AIDS-related illnesses since the start of the epidemic, including 1.1 million in 2015. Progress also has been made in preventing mother-to-child transmission of HIV and keeping mothers alive (Boone, Cook, & Wilson, 2016). In 2015, 77% of pregnant women living with HIV globally had access to antiretroviral medicines to prevent transmission of HIV to their babies; new HIV infections among children have declined by 50% since 2010. Data obtained from the Union Ministry of Health & Family Welfare (MH&FW) shows HIV infections have been on the rise among women. Of the 18 lakh HIV-positive cases reported between 2009 and 2016, two-thirds were women and six lakh of them were pregnant. More than one and a half lakh women contracted HIV in 2016 alone. A substantial number of these women were pregnant: 35 per cent in 2010, and 50 per cent in 2016. There's a steady and rapid rise that can be spotted. According to the National Rural Health Mission, the number of women who are HIV-positive has gone up from 80,000 in 2010 to 1.5 lakh in 2016. India had 2.1 million people living with HIV at the end of 2016, with new infections falling to 80,000 in 2016 from 150,000 in 2005, shows data from the UNAIDS Ending AIDS Report 2017 released in Paris on Thursday (Reddy, 2017).

1.2. Pathophysiology:

1.2.1. Structure

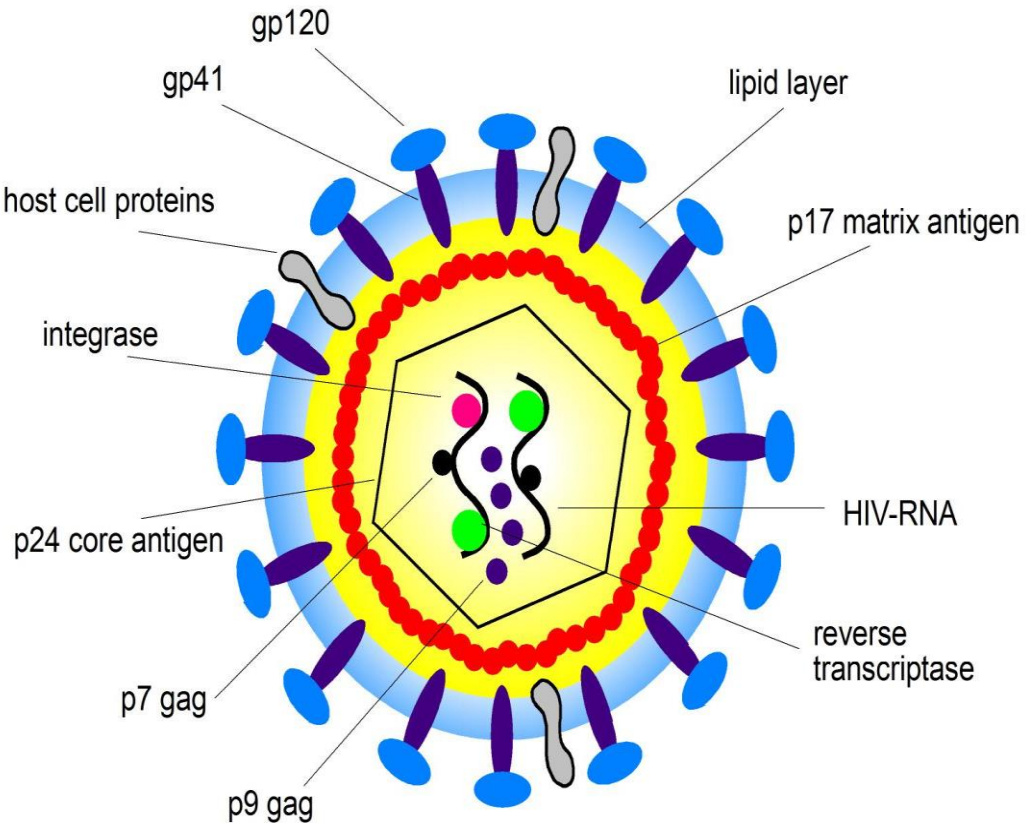

Figure 1.1 Structure of the HIV virus (taken from HIVbook.com)

Like other viruses, in HIV there is no cell wall and nucleus shown in **Figure 1.1**

The viral envelope: proteins which are embedded in the viral envelope is different, the outer coat of virus consists of two layer of lipids, forming "**spikes"** consisting of the outer glycoprotein (gp) 120 and trans membrane gp41 (Kwon et al., 2017).

During the budding process, the lipid membrane is borrowed from the host cell. Gp120 is needed to attach to the host cell, and for the cell fusion process gp41 is critical.

The HIV matrix proteins: envelop which is lie between the envelope and core of the virus.

The viral core, it contains the viral capsule proteins p24 (Jonathan Brostoff et al., 1998)

1.2.2. Life cycle of HIV virus:

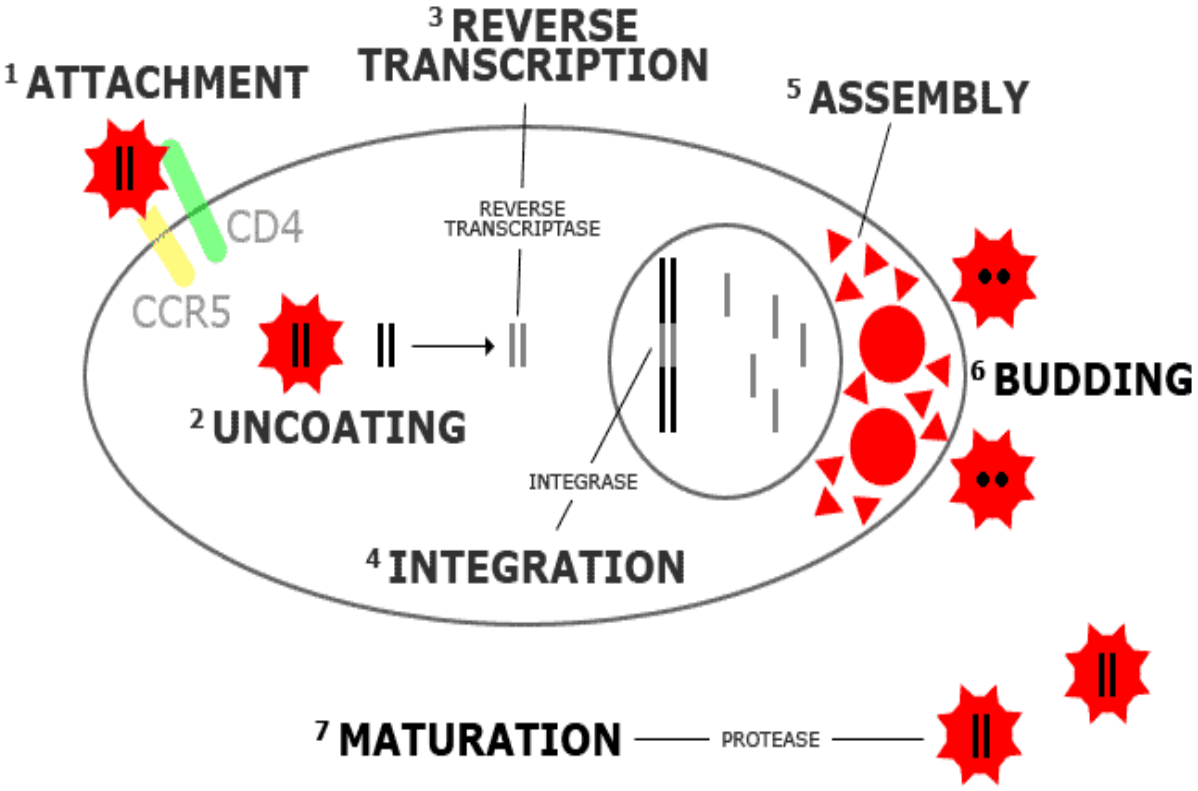

Figure 1.2 Life cycle of HIV (taken from https://studentreader.com/7TDLH/hiv/)

DIFFERENT STAGES OF HIV CYCLE:

1. **Free virus:**
2. **Attachment and entry:** Virus binds to a CD4 molecule and one type of "coreceptor" (either CCR5 or CXCR4). Receptor molecules are common on the cell surface. Then the virus fuses with the cell as shown in **Figure 1.2**
3. **Penetration:** after that, virus enters into cell.
4. **Reverse transcriptase:** It converts viral RNA to double-stranded DNA.
5. **Integration:** Viral DNA attached to the human DNA by the integrase enzyme.

6. **Transcriptase:** When the infected cell divides, the viral DNA is “read” and long chain of proteins are made.

7. **Assembly:** The newly formed HIV protein and HIV viral RNA move to the surface of the cell and form a viral chain.(Mailler et al., 2016)

8. **Budding:** Immature virus pushes out of the cell, taking some cell membrane with it. The protease enzyme starts processing the proteins in the newly forming virus (Pancera, Changela, & Kwong, 2017).

9. **Maturation:** The protease enzyme finishes cutting HIV protein chains into individual proteins. Then combine to form the viral core and make a new working virus. (Kirchhoff, 2013)

Causes: transmission of HIV-2 infectious agent by another person by one or more of the following: saliva, fecal-oral route, surfaces, blood, needles, blood transfusions, sexual contact, mother to fetus, etc.

Symptoms of HIV-1 infection: fever, body rashes, swollen throat, headache, stomach disturbance.

Symptoms of HIV-2 infection: weak immune system, low CD4+ count, persistently swollen lymph nodes, persistently tender lymph nodes, rapid weight loss.

1.3. Classification of anti-HIV agents:

There are 4 classes of Anti-HIV drugs:

1.3.1. Nucleoside reverse transcriptase inhibitors (NRTIs).

1.3.2. Non-nucleoside reverse transcriptase inhibitors (NNRTIs).

1.3.3. Protease inhibitors.

1.3.4. Fusion inhibitors.

1.3.1. Nucleoside reverse transcriptase inhibitors (NRTIs): Zidovudine, Stavudine, Didanosine, lamivudine, Abacavir.

1.3.2. Non-nucleoside reverse transcriptase inhibitors (NNRTIs): Nevirapine, Delavirdine, Efavirenz, Etravirine, Rilpivirine.

1.3.3. Protease inhibitors: ritonavir, Lopinavir, Saquinavir, Tipranavir.

1.3.4. Fusion inhibitors: Enfuvirtide.

Structure of anti-HIV inhibitors:

Structure of anti-HIV inhibitors are shown below in **Figure 1.3.**

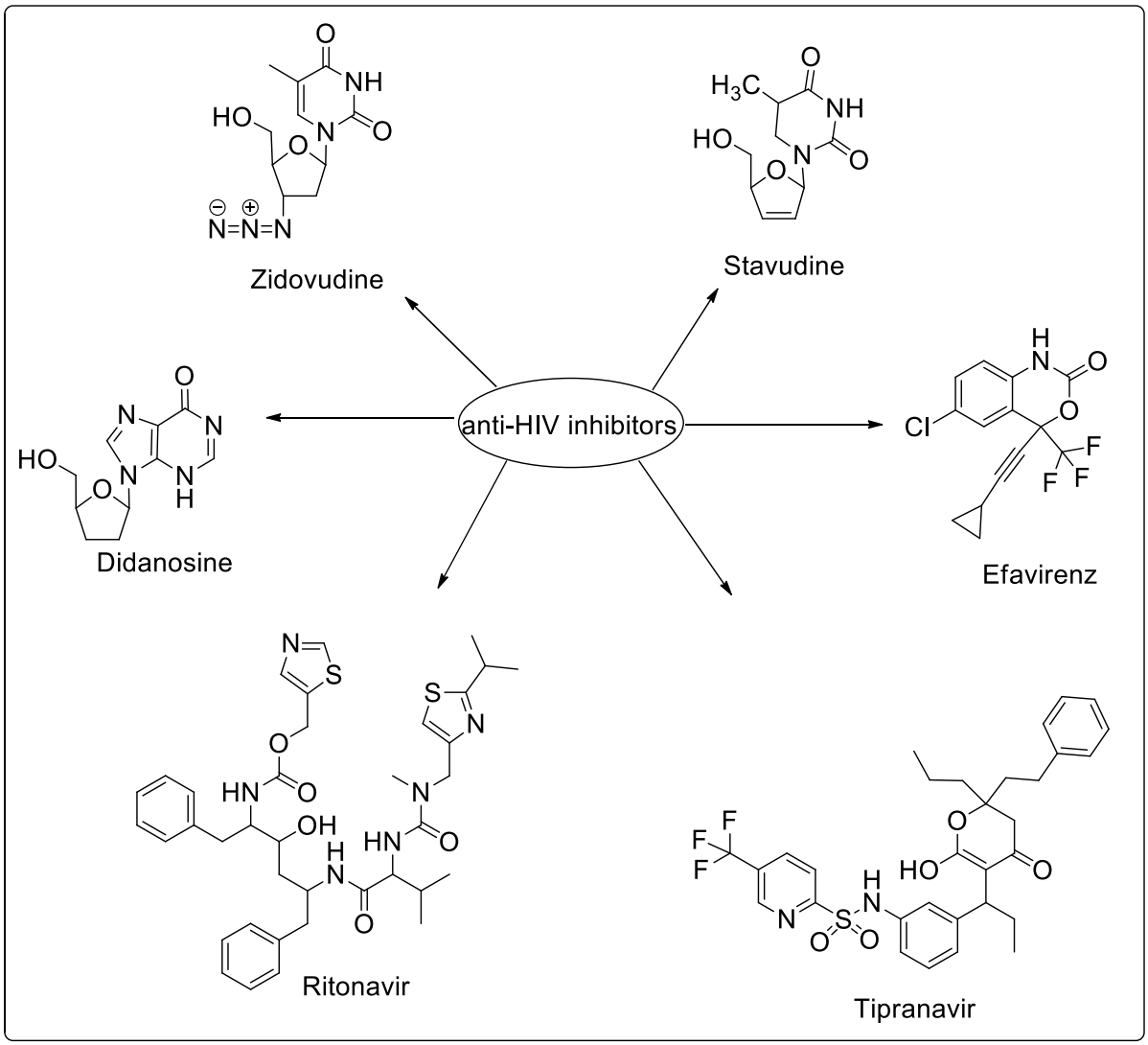

Figure 1.3 Structure of anti-HIV inhibitors

Chapter 2
LITERATURE REVIEW

2.1 Reverse transcriptase:

Howard Temin discovered Reverse transcriptase at the University of Wisconsin-Madison in RSV virions and David Baltimore in 1970 independently isolated at MIT from two RNA tumour viruses: R-MLV and again RSV. The reverse transcription of the viral single-stranded (+) RNA genome into double-stranded DNA (dsDNA) is an essential step in the replication of HIV (Samanta & Das, 2017). These enzymes are encoded and used by reverse transcribing viruses, which use the enzyme during the process of replication. Reverse-transcribing RNA viruses, such as retroviruses, use the enzyme to reverse-transcribe their RNA genomes into DNA, which is then integrated into the host genome and replicated along with it. Reverse-transcribing DNA viruses, such as the heap DNA viruses, can allow RNA to serve as a template in assembling and making DNA strands. HIV infects humans with the use of this enzyme. Without reverse transcriptase, the viral genome would not be able to incorporate into the host cell, resulting in failure to replicate (Kohlstaedt, Wang, Friedman, Rice, & Steitz, 1992). The structure of HIV-1 reverse transcriptase is shown in **Figure 2.1**

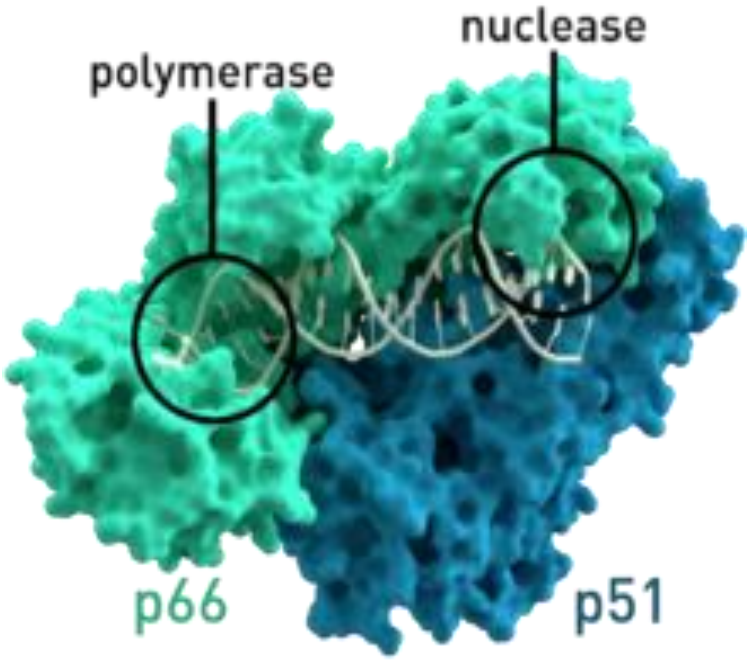

Figure 2.1 Crystal structure of wild-type HIV-1 Reverse Transcriptase **(taken from (Miller, Tuske, Das, DeStefano, & Arnold, 2016a)**

HIV RT is a multifunctional heterodimer of a 66-kDa molecular mass p66 subunit and a 51-kDa molecular mass p51 subunit that, as a proteolytic product of the

p66 subunit, has the same sequence but adopts a different conformation. DNA polymerase and RNase H catalytic activities are both conferred on the enzyme by the larger p66 subunit of the enzyme (Miller, Tuske, Das, DeStefano, & Arnold, 2016b).

The p66 subunit is the larger of the two subunits within HIV-1 reverse transcriptase. This subunit contains the finger, palm, thumb, and connection subdomains as well as the RNase H subdomain (Sharaf, Brereton, Byeon, Karplus, & Gronenborn, 2016). The p51 subunit is the smaller of the two subunits in HIV-1 reverse transcriptase. This subunit also contains the finger, palm, thumb and connection subdomains. The p51 subunit is a product of the same gene as the p66 subunit, however, the RNase H domain is absent in the p51 subunit as a result of proteolytic cleavage (Das et al., 2016). 3-D structure of HIV-1 RT is given in **Figure 2.2**

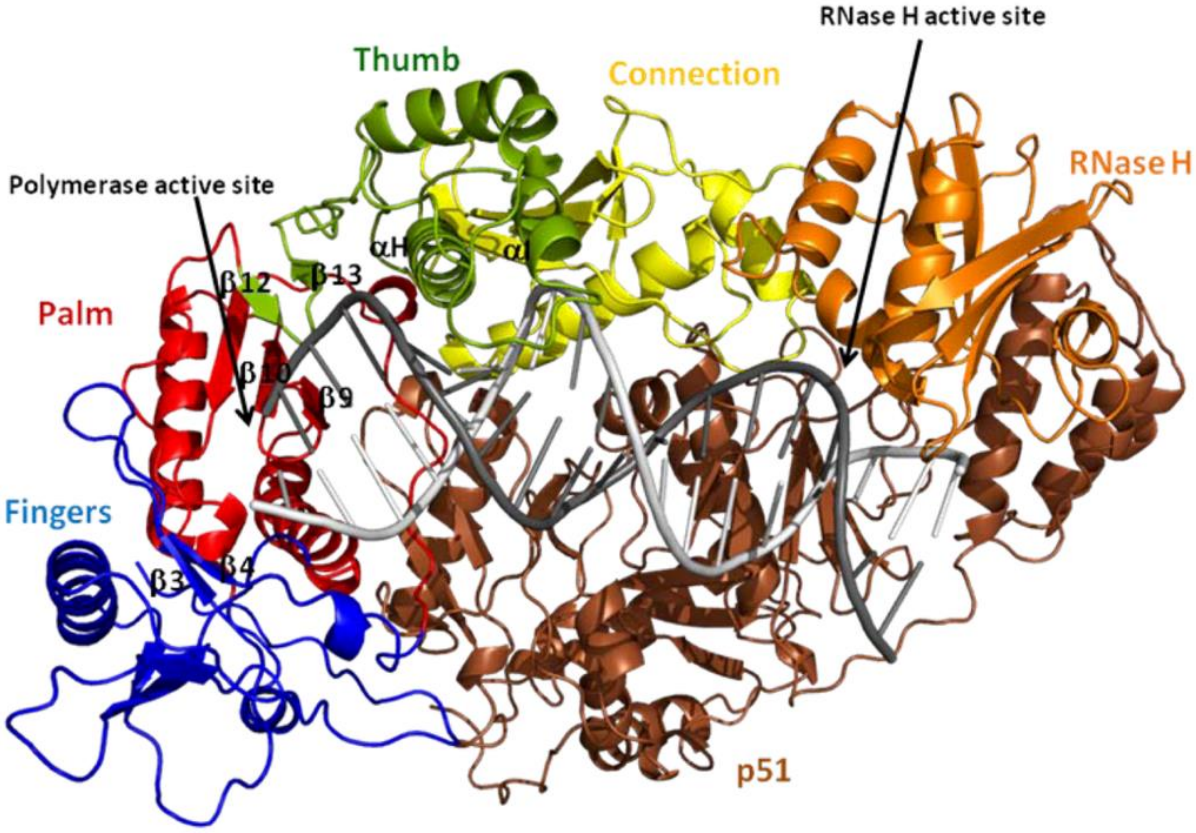

Figure 2.2 3-D structure of HIV-1 RT bound to double stranded DNA

HIV-1 RT functions as heterodimer of p66 and p51 subunits. Due to the resemblance of p66 to a closed right hand, subdomains of p66 have been

named as the ‘palm’ (red), fingers (blue), and thumb (green). The p66 subdomain contains two active sites, the polymerase and the RNase H active sites (orange) (Yamani et al., 2017). The region between the RNase H and polymerase active sites is known as the connection (yellow) subdomain. The p51 (dark brown) subunit is derived from the proteolytic cleavage of RNase H from p66 and has identical primary and secondary structure (Miller et al., 2016b). However, the tertiary structure of p51 is markedly different than p66 leading to a non-functional arrangement of catalytic residues. The template/primer (white/gray) is seen in the DNA-binding cleft formed primarily by the p66 subunit of the enzyme. (Sarafianos et al., 2009)

2.2 FDA approved Reverse transcriptase inhibitors:

Some FDA approved drugs are described below which are used as reverse transcriptase inhibitors.

2.2.1 Zidovudine:

Zidovudine is used to treat anti-HIV medication. It is in a category of HIV medications called nucleoside reverse transcriptase inhibitors (NRTIs). AZT works by selectively inhibiting HIV's reverse transcriptase, the enzyme that the virus uses to make a DNA copy of its RNA. Zidovudine prevents HIV from altering the genetic material of healthy T-cells(Faure, Paques, & Audo, 2017). This prevents the cells from producing new virus and decreases the amount of virus in the body. Zidovudine, manufactured by GlaxoSmithKline, was the first drug approved for the treatment of HIV, in 1987 (Mandala, Thompson, & Watts, 2016).

Side effects:

Bone marrow problems, such as decreased production of red blood cells and/or white blood cells, liver problems, feeling tired (fatigue), rash, trouble sleeping (insomnia), nausea, and headache can also be caused by Retrovir.

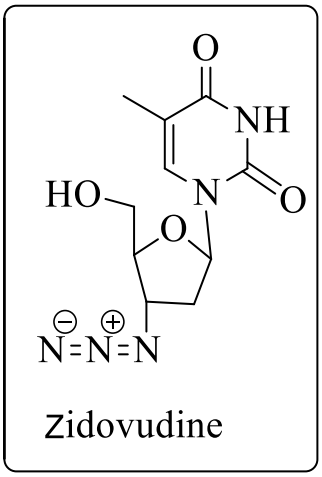

Zidovudine

2.2.2 Stavudine

Stavudine is a nucleoside analog of thymidine. It is phosphorylated by cellular kinases into an active triphosphate. Stavudine triphosphate inhibits HIV's reverse transcriptase by competing with the natural substrate, thymidine triphosphate. Reverse transcriptase is the enzyme the virus uses to make a DNA copy of its RNA in order to insert its genetic material into the host's DNA. Upon incorporation into the DNA strand, stavudine triphosphate causes termination of DNA replication (Ghosh, Mondal, Chakraborty, & Mukherjee, 2017).

Side effects:

These include nausea, vomiting, chills, fever, diarrhoea, constipation, headaches, abdominal pain and dehydration.

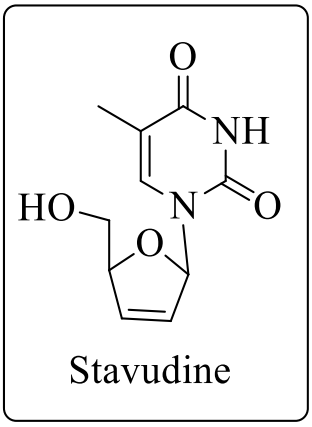

Stavudine

2.2.3 Didanosine

Videx is a trade name of Didanosine, is a medication used to treat HIV/AIDS. It is firstly described in 1975 and approved for use in the United States in 1991. It is used in combination with other medications as part of highly active antiretroviral therapy (HAART). It belongs to the reverse transcriptase inhibitor class. Didanosine was first described in 1975 and approved for use in the United States in 1991. Like other anti-HIV nucleoside analogs, it acts as a chain terminator by incorporation and inhibits viral reverse transcriptase by competing with natural dATP. Didanosine is a synthetic nucleoside analogue of the naturally occurring nucleoside deoxyadenosine in which the 3'-hydroxyl group is replaced by hydrogen. Intracellularly, didanosine is converted by cellular enzymes to the active metabolite, dideoxyadenosine 5'-triphosphate. Dideoxyadenosine 5'-triphosphate inhibits the activity of HIV-1 reverse transcriptase both by competing with the natural substrate, deoxyadenosine 5'-triphosphate, and by its incorporation into viral DNA causing termination of viral DNA chain elongation (Penkalski, Felicilda-Reynaldo, & Patterson, 2017).

Side effects:

The most common adverse events with didanosine are diarrhea, nausea, vomiting, abdominal pain, fever, headache and rash.

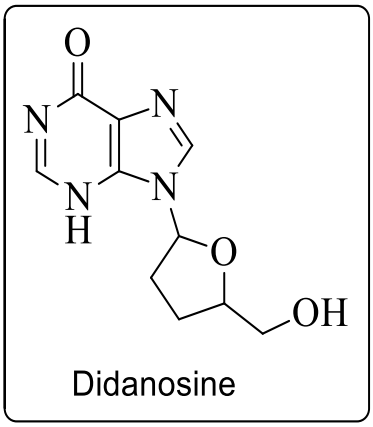

Didanosine

2.2.4 Lamivudine

Lamivudine is a type of drug called a nucleoside reverse transcriptase inhibitor (NRTI). They inhibit the HIV reverse transcriptase enzyme competitively and act as a chain terminator of DNA synthesis. The lack of a 3'-OH group in the incorporated nucleoside analogue prevents the formation of the 5' to 3' phosphodiester linkage essential for DNA chain elongation, and therefore, the viral DNA growth is terminated (Prevedel, Morocho, Bennett, & Eugenin, 2017).

Side effects: The common side effects that can occur with lamivudine include changes in the distribution of fat on your body, such as an increasing amount of fat on your neck and back, cough, diarrhea, fatigue, headache, malaise (general discomfort), nasal symptoms, such as a runny nose and nausea.

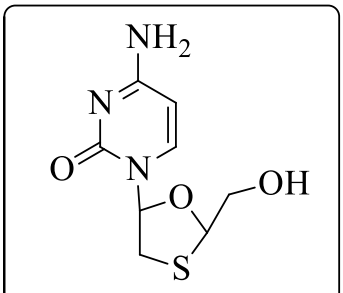

Lamivudine

2.2.5 Delavirdine

Delavirdine is a Human Immunodeficiency Virus 1 Non-Nucleoside Analog Reverse Transcriptase Inhibitor. It is used to inhibit the conversion of single strand viral RNA into double strand viral DNA. The chemical classification of delavirdine is Non-Nucleoside Analog. Delavirdine is a synthetic, non-nucleoside reverse transcriptase inhibitor. In combination with other anti-retroviral drugs, this agent has been shown to reduce HIV viral load and increase CD4 leukocyte counts in patients.(Ntshongontshi et al., 2016)

Side effects:

Signs of an infection such as fever, chills, night sweats, sore throat, flu symptoms, weakness, easy bruising or unusual bleeding, loss of appetite, mouth sores; rapid heart rate, tremors, sleep problems (insomnia), feeling anxious or irritable.

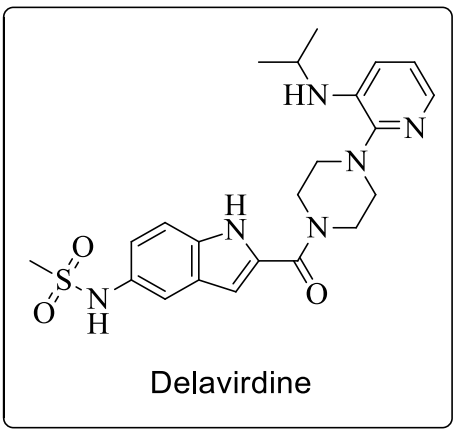

Delavirdine

2.2.6 Efavirenz

Efavirenz is an intense, non-nucleoside reverse-transcriptase inhibitor, discovered at Merck research Laboratories. It is utilized as a major aspect of exceptionally dynamic antiretroviral therapy (HAART) for the treatment of a human immunodeficiency virus (HIV) type 1. Efavirenz was approved by the FDA on 1998, making it the fourteenth approved the antiretroviral drug.(Mandala et al., 2016)

Side effects: Mild nausea, vomiting, or stomach pain, diarrhea or constipation, cough, blurred vision, headache, tired feeling, dizziness, spinning sensation, problems with balance or coordination, muscle or joint pain, sleep problems (insomnia), unusual dreams.

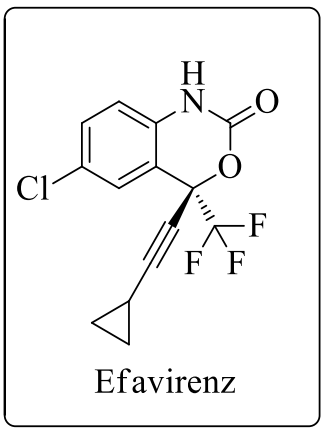

Efavirenz

2.2.7 Elvitegravir

Elvitegravir is a prescription medicine approved by the U.S. Food and Drug Administration (FDA) for the treatment of HIV infection in adults who are already taking or have taken HIV medicines before. Elvitegravir is always used in combination with other HIV medicines.

Elvitegravir belongs to a class (group) of HIV drugs called integrase inhibitors. Integrase inhibitors block an HIV enzyme called integrase. (An enzyme is a protein that starts or increases the speed of a chemical reaction.) By blocking integrase, integrase inhibitors prevent HIV from multiplying and can reduce the amount of HIV in the body (Best, Capparelli, & Stek, 2017).

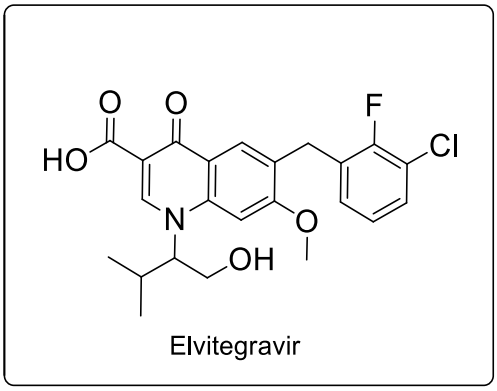

Elvitegravir

2.3 Quinoline

Quinoline or 1-aza-napthalene or benzo[b]pyridine is nitrogen containing heterocyclic aromatic compound. It has a molecular formula of C9H7N and its molecular weight is 129.16. The log P value is 2.04 and has an acidic pKb of 4.85 and a basic pKa of 9.5. Quinoline is a weak tertiary base. It can form salt with acids and displays reactions similar to those of pyridine and benzene. It shows both electrophilic and nucleophilic substitution reactions. It is nontoxic to humans on oral absorption and inhalation.

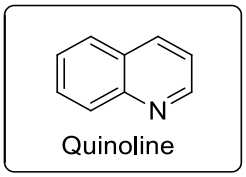

Quinoline

Quinoline nucleus occurs in several natural compounds (Cinchona Alkaloids) and pharmacologically active substances displaying a broad range of biological

activity such as antimalarial (Patel, Patel, & Chikhalia, 2018), anti-inflammatory (Srilakshmi & Adapa, 2017), antifungal (Liu et al., 2017), analgesic activity (Gupta & Mishra, 2016), anti-bacterial (Parekh, Maheria, Patel, & Rathod, 2011), cardio tonic , anthelmintic (Anitha, Sreenivasa, Mohan, Chandramohan, & Shivaraja, 2017), anticonvulsant (Kedjadja, Bouraiou, & Merdes, 2018). Shown in **figure 2.3**

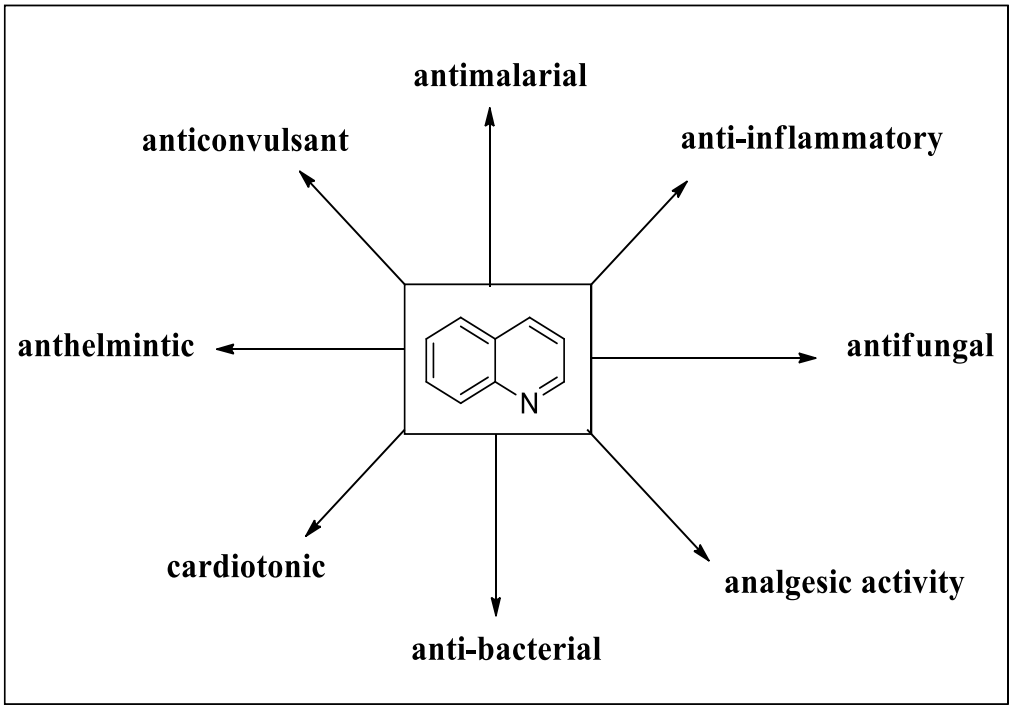

Figure 2.3 Medicinal applications of quinoline

2.3.1 Quinoline derivatives as anti-HIV agents:

Quinoline moiety is present in many classes of biologically active compounds. Quinoline derivatives have also shown anti-HIV reverse transcriptase activities. Elvitegravir and efavirenz are the FDA approved quinoline containing HIV reverse transcriptase inhibitors.

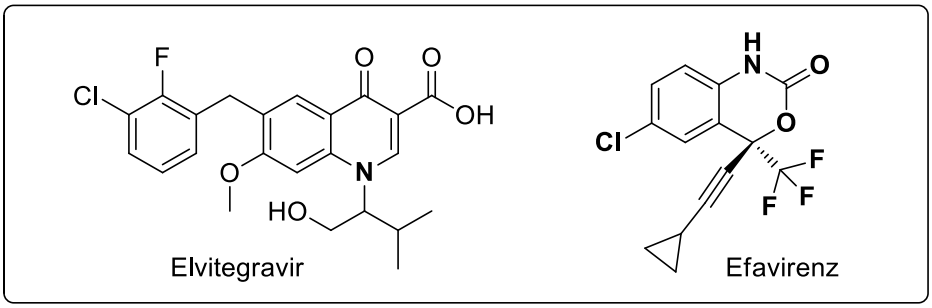

Many quinoline derivatives are reported to have HIV reverse transcriptase inhibitory activity. HIV reverse transcriptase inhibitors containing quinoline moiety are summarized in **Table 2.1**

Table 2.1: Quinoline derivatives are reported to have HIV reverse transcriptase inhibitors

S.No.	Structure	IC_{50} (µM)	Reference
1.	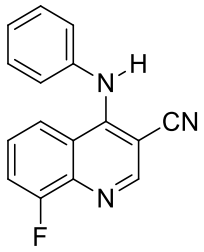	<8	(Melo et al., 2017)
2.	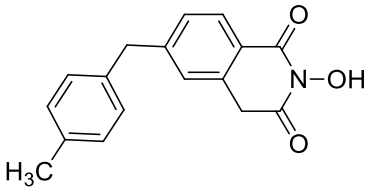	1.2 ± 0.1	(Cai, Liu, & Chen, 2018)
3.	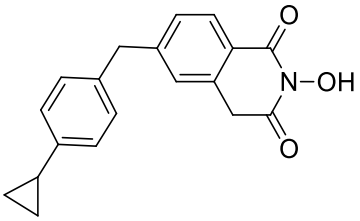	0.60 ± 0.1	(Cai et al., 2018)
4.	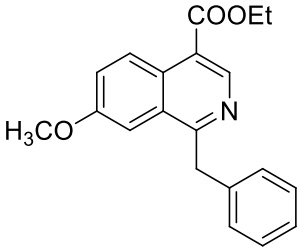	~10	(George, Gopi Krishna Reddy, Satyanarayana, & Raghavendra, 2018)
5.	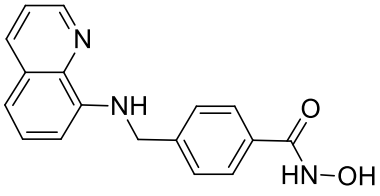	0.29 nM	(Lee et al., 2018)

2.4 Pyrazoline

Pyrazoline are an important class of heterocyclic compounds containing two nitrogen atoms in the five membered ring. The substituted 2-pyrazolines have found application as activators for polymerization. Pyrazoline derivatives are the electron rich nitrogen heterocycles which play an important role in the diverse biological activities. These heterocyclic compounds widely occur in nature in the form of alkaloids, vitamins, pigments and as constituents of plant and animal cell.

These compounds have been found to possess anti-fungal (Manivannan & Santhi, 2017), anti-depressant (Sowmya et al., 2017), anticonvulsant (Beyhan, Kocyigit-Kaymakcioglu, Gümrü, & Aricioglu, 2017), anti-inflammatory (Shringare et al., 2018), anti-bacterial (Mahmoodi, Zeydi, Mamaghani, & Montazeri, 2017) and anti-tumor (Gangarapu et al., 2017) properties are shown in **Figure 4.2**. The pyrazole moiety is found in blockbuster drugs such as celecobix, sildenafil and rimonabant (Yusuf & Jain, 2014).

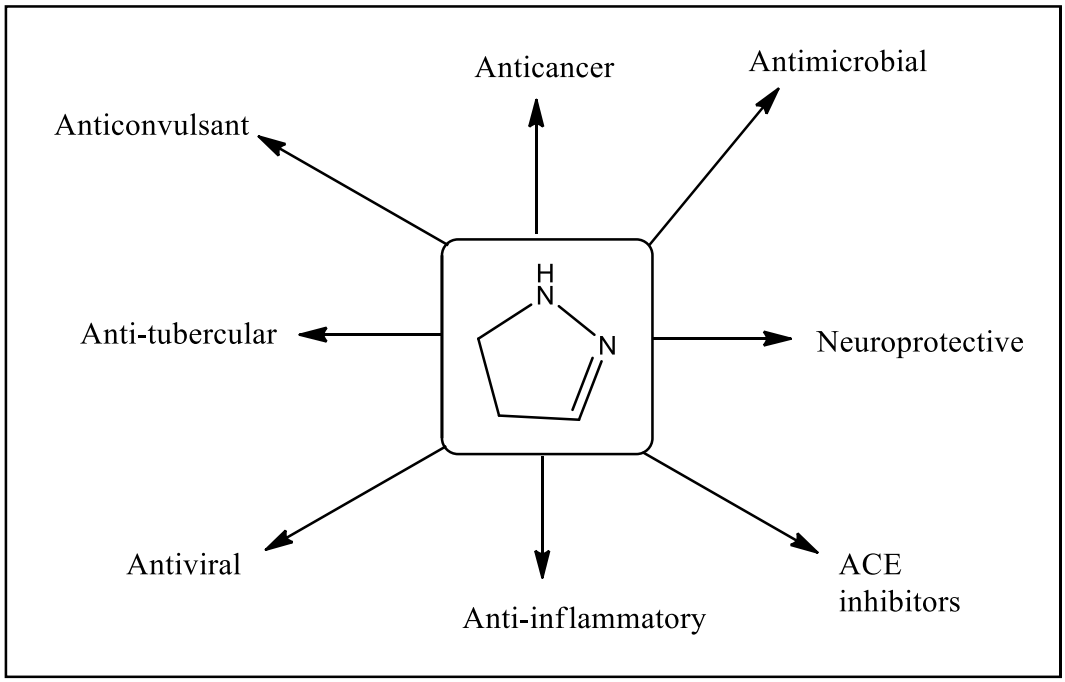

Figure 2.4. Medicinal applications of Pyrazoline derivatives

CHAPTER 3

RATIONALE

3.0 Rationale

Reverse transcriptase plays crucial role in the conversion of viral single strand RNA into viral double strand DNA. It emerged as an important target which needs to be inhibited to stop the conversion of viral RAN into viral DNA and treatment of HIV. From the review of literature it is clear that the drawback of currently available anti-HIV inhibitors is in effectiveness in the treatment. Side effects like Bone marrow problems, such as decreased production of red blood cells and/or white blood cells, liver problems, feeling tired (fatigue), rash are mainly due to their irreversible binding with the target. Problems related to anti-HIV drugs can be addressed by designing targeted drugs that are able to inhibit the reverse transcriptase which converts the viral single strand RNA into viral double strand DNA with lesser side effects. From exploration of the crystal structure of reverse transcriptase it has been established that pocket of reverse transcriptase interacts mainly with two subunits p51 and p66, where the p66 subunit is the larger of the two subunits within HIV-1 reverse transcriptase. This subunit contains the finger, palm, thumb, and connection subdomains as well as the RNase H subdomain. The p51 subunit is the smaller of the two subunits in HIV-1 reverse transcriptase. This subunit also contains the finger, palm, thumb and connection subdomains. Therefore, the aim of this project was to design and synthesize pyrazoline containing quinoline derivatives as reverse transcriptase inhibitors.

3.1 Design of proposed molecules

The design of our compounds was done by taking Elvitegravir and Capravirine as reference compounds as follows:

1. Capravirine containing imidazole ring which was replaced with Pyrazoline ring.
2. With reference of Elvitegravir Quinoline moiety is introduced in our compound and chlorine is used.
3. Benzene ring with different substitution was taken from Elvitegravir and Capravirine.

The above mentioned points are summarized in **Figure 3.1.**

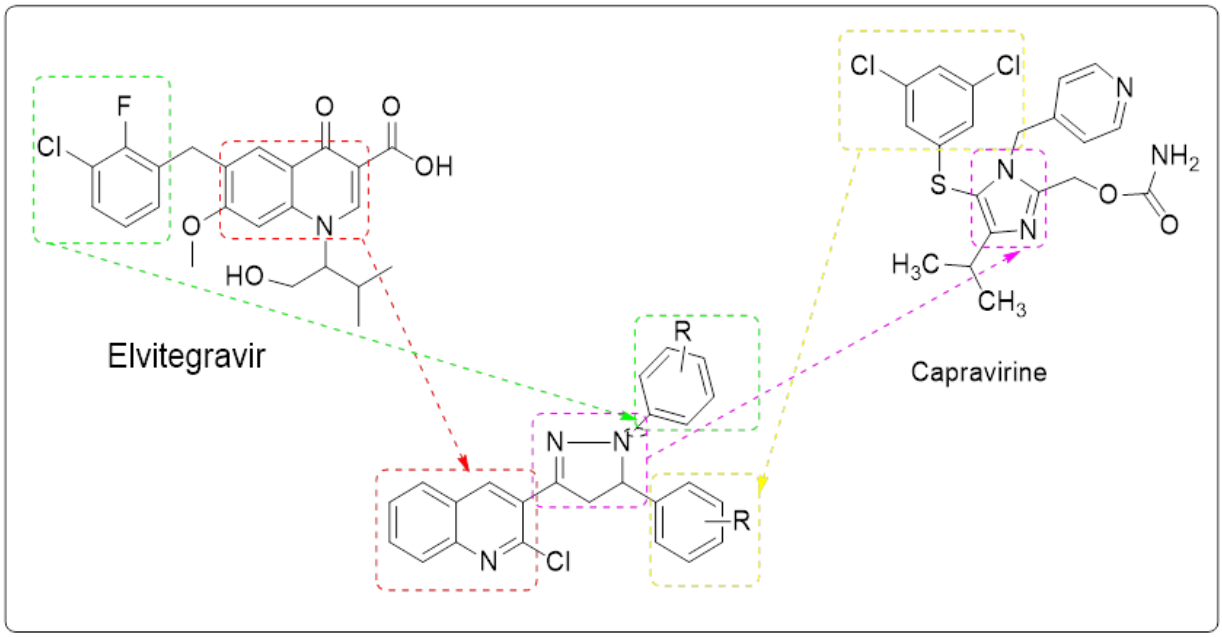

Figure 3.1 shows the design of proposed molecule

3.2 Design of compounds by docking

Docking studies of proposed compounds and standard inhibitor elvitegravir revealed that the proposed compound binds at the same cavity where the standard inhibitor was bound.

The overlapping of proposed compound and standard inhibitor elvitegravir is shown in **Figure 3.2.**

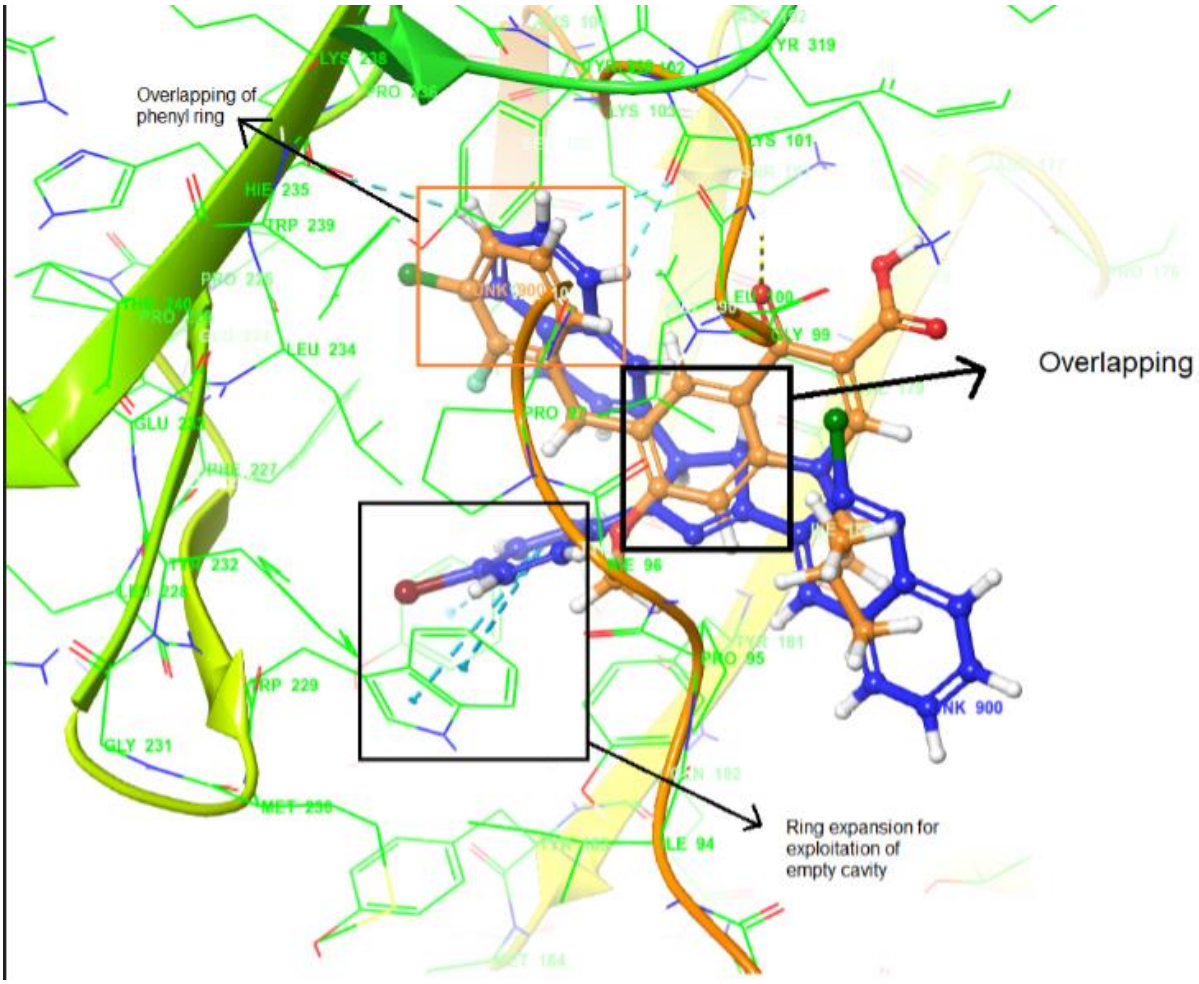

Figure 3.2. 3-D interaction of proposed molecule and standard inhibitor, orange- Standard inhibitor, blue-Proposed molecule

CHAPTER 4

OBJECTIVES

4.0 Objectives

With this literature background we set the following objectives:

1. Design and synthesis of purposed compounds pertaining to structure given below:

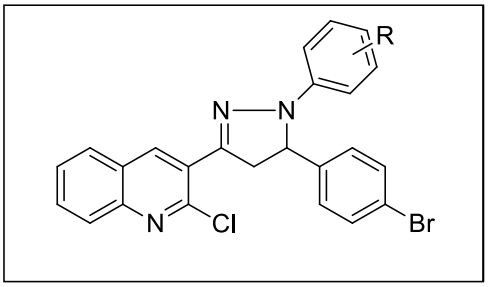

2. Docking study of the compounds into active site of the target protein (PDB Id: 4I2P)

CHAPTER 5

MATERIALS AND METHODS

5.0. Materials and Methods

5.1. General:

1. All the reagents and solvents were purchased from Sigma-Aldrich, Loba-Chemie Pt. Ltd., S.D.F.C.L., Sisco Research Laboratory and HiMedia Laboratories Ltd. (AR/GR quality) and were used without further purification.

2. Sartorius analytical balance (BSA224s-CW) was used for the weighing purposes.

3. JSGW heating mantle for reflux reactions and ILMVAC rotary evaporator, were used for drying the organic compounds.

4. The progress of the reactions was monitored by TLC, using either petroleum ether/ethyl acetate or chloroform/methanol as the mobile phase on pre-coated Merck TLC plates in JSGW UV/fluorescent analysis cabinet and/or iodine chamber.

5. Melting points were recorded on Stuart melting point apparatus (SMP-30) with open glass capillary tube and are uncorrected.

6. Compounds were purified using column chromatography (Biotage) (Unless otherwise stated, chromatography was conducted using high-purity grade, pore size 60 Å, 220-440 mesh particle size, 35-75 µm particle size, Silica, to obtain the pure desired product).

7. IR spectra of compounds were recorded with KBr on a Bruker FT-IR spectrophotometer.

8. NMR experiments were performed at Ropar (Punjab, India). ^{1}H NMR and ^{13}C NMR spectra were obtained in CDCl3/d6-DMSO on 400 MHz and 100 MHz Bruker Advance II NMR spectrometer, respectively using TMS (δ = 0) as an internal standard.

5.2 Synthesis of intermediates

5.2.1 Procedure for the synthesis of starting material 2-chloroquinoline-3-carbaldehyde (DCS-1)

$POCl_3$ (1.5 mL, 98.28 mmol) was added drop wise via dropping funnel to DMF (0.45 mL, 34.65 mmol) at 0-5 °C, mixture was stirred for about 5 min. Acetanilide (0.236 g, 10.37 mmol) was then added to the reaction mixture and the resulting solution was heated for 8 h (75- 80 °C) are shown in **Figure 5.1**.

The reaction mixture was cooled to r.t. and then poured into crushed ice with stirring. A precipitate appeared at once, which was filtered, washed with H_2O and dried. The crude compound was then recrystallized from EtOAc.

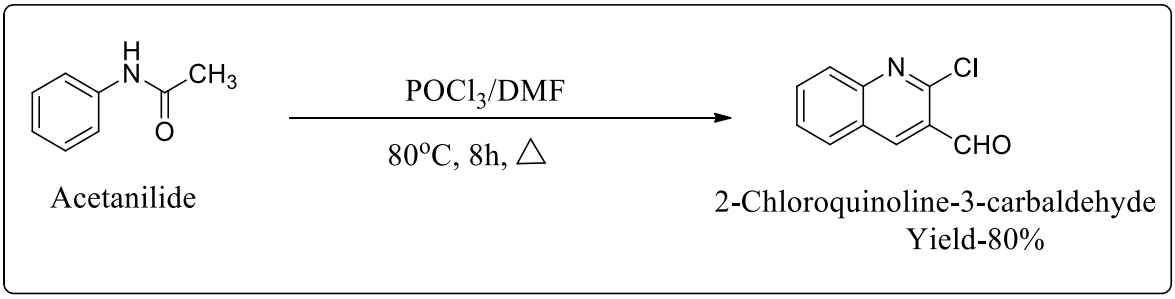

Figure 5.1 Reaction for the synthesis of DCS-1

5.2.1.1 2-chloroquinoline-3-carbaldehyde (DCS-1)

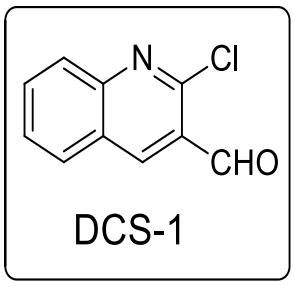

Pale-yellow precipitate

Yield = 80%. MP: 142-144°C. IR (KBr) cm^{-1}: C=N Stretch (2360), Aldehyde C=O Stretch (1686.82), C-Cl stretch (761.06), C-N stretch (1046.20), C=C stretch (1614.14)

^{1}H NMR ($CDCl_3$, 400 MHz, δ with TMS = 0): 7.65 (1H, t, J = 8 Hz), 7.89 (1H, t, J = 12 Hz), 7.97 (1H, d, J = 8 Hz), 8.06 (1H, d, J = 8 Hz), 8.73 (1H, s), 10.53 (1H, s).

^{13}C NMR (100 MHz, $CDCl_3$) δ: 189.26, 150.18, 149.64, 140.39, 133.72, 129.82, 128.67, 128.24, 126.59, 126.41.

Mass (EI): Calculated for $C_{10}H_6ClNO$: 191.01 $[M]^+$; found 191, [M+2] peak at 193 (Due to chlorine).

5.2.2 Synthesis of chalcones

5.2.2.1: (E)-1-(4-bromophenyl)-3-(2-chloroquinolin-3-yl)prop-2-en-1-one(DCC-2)

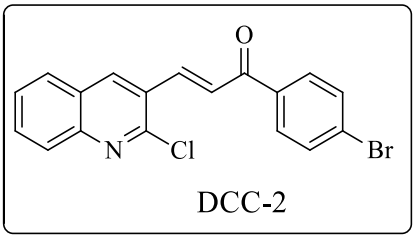

DCC-2

2-chloroquinoline-3-carbaldehyde (0.1g) was added to 4-bromo-acetonapthone (0.089g). After adding 5 ml methanol, the mixture was stirred until the reactants got completely dissolved. 5 ml of 20% NaOH was then added to it. Reaction mixture was stirred for 4-5 h and precipitates appeared which were filtered, washed with water, dried and recrystallized using methanol. Reaction was monitored by TLC using petroleum ether: ethyl acetate (7:3).

Yield: 70%, pale yellow crystals, **m.p.** 172 – 176 ^{o}C. IR (KBr) cm^{-1}: Nitrile C=N Stretch (2360), Ketone C=O Stretch (1671.14), C-Cl stretch (746.83), C-N stretch (1044.55), C=C stretch (1655.37), C-Br stretch (750)

Mass (EI): calculated for $C_{18}H_{11}BrClNO$: 370.97 [M^{+}]; found: 370, [M+2] peak at 372.

^{1}H NMR ($CDCl_3$, 400MHz, δ with TMS = 0): 7.58 (1H, s), 7.62 (1H, m), 7.65 (2H, m), 7.80 (1H, m), 7.88 (1H, d, J = 8 Hz), 7.91 (2H, d, J = 4 Hz), 8.02 (1H, d, J = 8 Hz), 8.20 (1H, d, J = 16 Hz), 8.48 (1H, s).

^{13}C NMR (100 MHz, $CDCl_3$) δ 188.8, 150.4, 148.0, 140.0, 136.4, 132.2, 132.1, 131.8, 130.2, 129.5, 128.6, 128.5, 128.2, 128.1, 128.0, 127.8, 127.0, 125.8

Mass (EI): Calculated for $C_{18}H_{12}BrClNO$: 370 $[M]^{+}$, [M+2] peak at 372.

5.2.3 Synthesis of final compounds

5.2.3.1: 3-(1-(4-bromophenyl)-5-(naphthalen-2-yl)-4,5-dihydro-1H-pyrazol-3-yl)-2-chloroquinoline (DC-1)

DCC-2 (200mg) was added to 4-bromo phenyl Hydrazine hydrochloride (3 Eq.). After adding 5 ml methanol the mixture were stirred until the reactants was completely dissolved. Reaction was stirred on magnetic stirrer for 4-5 h at 50^{o}C-60^{o}. Reaction was being monitored by TLC pet ether: ethyl acetate (7:3). After 4 hours, yellow colored precipitates appeared which were filtered and washed with water. Filtered precipitates were dried and purified by column chromatography, recrystallized by methanol and DCM.

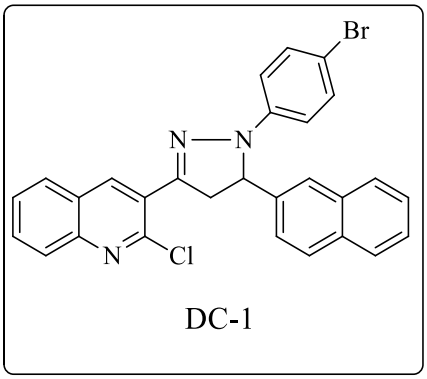

DC-1

Yield: 75%, greenish yellow crystals, **m.p.** 210 – 215 ^{o}C.

^{1}H NMR ($CDCl_3$, 400 MHz, δ with TMS = 0): 3.33 (1H, dd, J_{12} = 8Hz, J_{13} = 4 Hz), 4.25 (1H, dd, J_{12} = 13 Hz, J_{13} = 20 Hz), 5.75 (1H, dd, J_{12} = 4 Hz, J_{13} = 12 Hz), 6.97 (2H, m), 7.30 (2H, m), 7.45 (1H, m), 7.47 (1H, d, J = 4 Hz), 7.48 (1H, m), 7.69 (1H, m), 7.70 (1H, m), 7.80 (1H, m), 7.81 (1H, m), 7.82 (1H, m), 7.83 (1H, s), 7.92 (1H, s), 8.04 (1H, d, J = 8 Hz), 8.14 (1H, d, J = 8 Hz).

^{13}C NMR (100 MHz, $CDCl_3$) δ 148.68, 148.20, 147.32, 143.06, 135.98, 135.13, 133.74, 133.30, 131.98, 130.89, 129.87, 129.62, 128.50, 128.40, 128.27, 127.99, 127.92, 127.86, 127.62, 127.34, 126.85, 126.77, 125.81,125.10, 124.41, 123.39, 114.93, 111.91.

Mass (EI): calculated for $C_{28}H_{19}BrClN_3$ $[M]^{+}$; 511.05; found 511, [M+1] peak at 510 (due to chlorine and bromine).

5.2.3.2 3-(5-(4-bromophenyl)-1-(3-fluorophenyl)-4,5-dihydro-1H-pyrazol-3-yl)-2-chloroquinoline (DC-4)

DCC-2 (200mg) was added to 3-fluoro phenyl Hydrazine hydrochloride (3 Eq.). After adding 5 ml methanol the mixture were stirred until the reactants was completely dissolved. Reaction was stirred on magnetic stirrer for 4-5 h at 50^{o}C-60^{o}. Reaction was being monitored by TLC pet ether: ethyl acetate (7:3). After 4 hours, yellow colored precipitates appeared which were filtered and washed with water. Filtered precipitates were dried and purified by column chromatography, recrystallized by methanol and DCM.

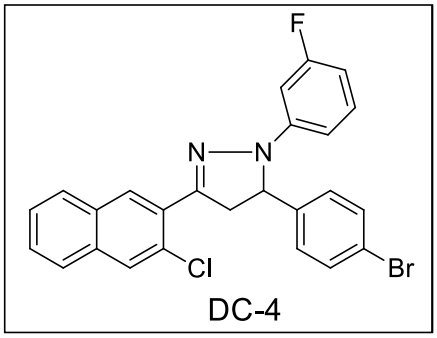

DC-4

Yield: 57.14 %, yellowish green, **m.p.** 215 – 218 ^{o}C.

^{1}H NMR ($CDCl_3$, 400 MHz, δ with TMS=0): 3.14 (1H, dd, J_{12} = 4 Hz, J_{13} = 16Hz), 4.07 (1H, dd, J_{12} =12 Hz, J_{13} = 20 Hz), 5.70 (1H, m), 6.54 (1H, m), 6.68 (1H, s), 7.12 (1H, m), 7.51 (1H, m), 7.52 (2H, d, J = 4 Hz), 7.58 (1H, s), 7.60 (2H, d, J = 8 Hz), 7.69 (1H, d, J = 8 Hz), 7.72 (1H, d, J = 4 Hz), 7.92 (1H, s), 8.02 (1H, d, J = 8 Hz).

^{13}C NMR (100 MHz, $CDCl_3$) δ 165.06, 162.64, 148.56, 147.32, 147.22, 136.01, 135.91, 131.95, 130.93, 127.97, 127.64, 127.47, 108.61, 108.60, 106.46, 101.11, 100.84, 77.42, 77.10, 76.78, 61.42, 58.97, 42.29, 42.23.

Mass (EI): calculated for $C_{24}H_{16}BrClFN_3$ 479.02; found 479 [M+2] peak at 481.

5.2.3.3 3-(5-(4-bromophenyl)-1-(3-chlorophenyl)-4,5-dihydro-1H-pyrazol-3-yl)-2-chloroquinoline(DC-5)

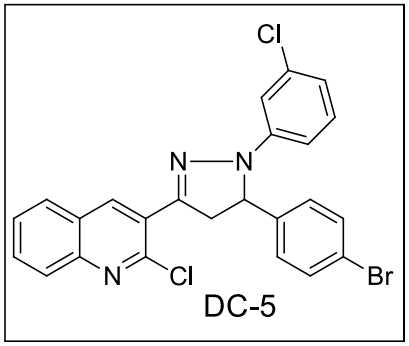

DC-5

DCC-2 (200mg) was added to 3-chloro phenyl Hydrazine hydrochloride (3 Eq.). After adding 5 ml methanol the mixture were stirred until the reactants was completely dissolved. Reaction was stirred on magnetic stirrer for 4-5 h at 50^{o}C-60^{o}. Reaction was being monitored by TLC pet ether: ethyl acetate (7:3). After 4 hours, yellow colored precipitates appeared which were filtered and washed with water. Filtered precipitates were dried and purified by column chromatography, recrystallized by methanol and DCM.

Yield: 65 %, Light green, **m.p.** 218 - 220 ^{o}C.

^{1}H NMR ($CDCl_3$, 400 MHz, δ with TMS = 0): 3.14 (1H, dd, J_{12} = 4 Hz, J_{13} = 16 Hz), 4.07 (1H, dd, J_{12} = 4 Hz, J_{13} = 16 Hz), 5.72 (1H, dd, J_{12} = 8 Hz, J_{13} = 12 Hz), 6.68 (1H, dd, J = 4 Hz), 6.80 (1H, dd, J = 4 Hz), 7.06 (1H, t, J = 8 Hz), 7.24 (1H, t, J = 4 Hz), 7.53 (1H, s), 7.51 (2H, m), 7.60 (2H, m), 7.71 (2H, m), 7.88 (1H, s), 8.03 (1H, d, J = 12 Hz).

^{13}C NMR (100 MHz, $CDCl_3$) δ 158.6, 135.8, 132.0, 131.9, 131.8, 130.9, 130.32, 128.25, 127.98, 127.86, 127.65, 127.49, 119.84, 113.64, 111.02, 108.21, 107.4, 61.25, 42.3, 32.0, 29.7, 29.7, 14.2.

Mass (EI): Calculated for $C_{24}H_{16}BrCl_2N_3$ $[M]^{+}$; 494.99; found 494, [M+2] peak at 497.

5.2.3.4 3-(1,5-bis(4-bromophenyl)-4,5-dihydro-1H-pyrazol-3-yl)-2-chloroquinoline (DC-6)

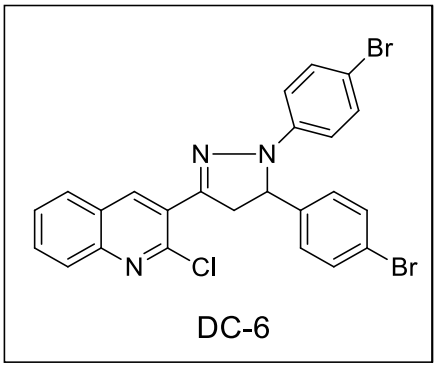

DC-6

DCC-2 (200mg) was added to 4-bromo phenyl Hydrazine hydrochloride (3 Eq.). After adding 5 ml methanol the mixture were stirred until the reactants was completely dissolved. Reaction was stirred on magnetic stirrer for 4-5 h at 50^{o}C-60^{o}. Reaction was being monitored by TLC pet ether: ethyl acetate (7:3). After 4 hours, yellow colored precipitates appeared which were filtered and washed with water. Filtered precipitates were dried and purified by column chromatography, recrystallized by methanol and DCM.

Yield: 60 %, Dark green, **m.p.** 219 - 222 ^{o}C.

^{1}H NMR ($CDCl_3$, 400 MHz, δ with TMS = 0): 3.15 (1H, dd, J = 8 Hz), 4.08 (1H, dd, J_{12} = 12 Hz, J_{13} = 16 Hz), 5.70 (1H, dd, J_{12} = 8 Hz, J_{13} = 12 Hz), 6.89 (2H, d, J = 8 Hz), 7.29 (2H, d, J = 8 Hz), 7.52 (2H, d, J_{23} = 8 Hz), 7.50 (1H, d, J = 8 Hz), 7.59 (2H, d, J = 8 Hz), 7.72 (1H, m), 7.68 (1H, m), 7.87 (1H, s), 8.02 (1H, d, J = 8 Hz).

^{13}C NMR (100 MHz, $CDCl_3$) δ 148.5, 147.3, 147.1, 147.0, 147.3, 147.5, 147.7, 142.9, 135.9, 135.7, 135.6, 135.5, 135.9, 131.9, 131.8, 130.9, 128.3, 127.9, 127.6, 127.4, 123.4, 114.9, 112.1, 42.28.

Mass (EI): Calculate for $C_{24}H_{16}Br_2ClN_3$ $[M]^+$; 538.94; found 538, [M+2] peak at 541.

5.2.3.5 5-(4-bromophenyl)-3-(3-chloronaphthalen-2-yl)-1-(4-fluorophenyl)-4,5-dihydro-1H-pyrazole (Dc-10)

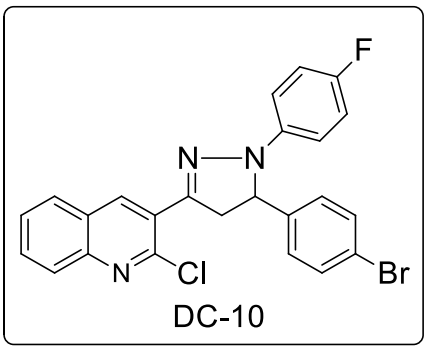

DC-10

DCC-2 (200mg) was added to 4-fluoro phenyl Hydrazine hydrochloride (3 Eq.). After adding 5 ml methanol the mixture were stirred until the reactants was completely dissolved. Reaction was stirred on magnetic stirrer for 4-5 h at 50^{o}C-60^{o}. Reaction was being monitored by TLC pet ether: ethyl acetate (7:3). After 4 hours, yellow colored precipitates appeared which were filtered and washed with water. Filtered precipitates were dried and purified by column chromatography, recrystallized by methanol and DCM.

Yield: 70%, green, **m.p.** 216 – 221 ^{o}C.

^{1}H NMR: ($CDCl_3$, 400 MHz, δ with TMS = 0) 3.12 (1H, dd, J = 8 Hz), 4.06 (1H, t, J = 12 Hz), 5.67 (1H, t, J = 8 Hz), 6.94 (4H, dd, J = 4 Hz), 7.50 (3H, d, J = 8 Hz), 7.58 (2H, d, J = 8 Hz), 7.72 (2H, m), 7.95 (1H, s), 8.05 (1H, d).

Mass (EI): Calculated for $C_{24}H_{16}BrClFN_3$: 479.02; found 479, [M+2] peak at 481 (Due to chlorine).

5.2.3.6 3-(1-(3-bromophenyl)-5-(4-bromophenyl)-4,5-dihydro-1H-pyrazol-3-yl)-2-chloroquinoline (DC-11)

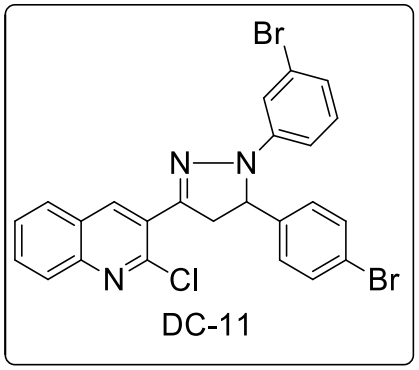

DC-11

DCC-2 (200mg) was added to 3-bromo phenyl Hydrazine hydrochloride (3 Eq.). After adding 5 ml methanol the mixture were stirred until the reactants was completely dissolved. Reaction was stirred on magnetic stirrer for 4-5 h at 50^{o}C-60^{o}. Reaction was being monitored by TLC pet ether: ethyl acetate (7:3). After 4 hours, yellow colored precipitates appeared which were filtered and washed with water. Filtered precipitates were dried and purified by column chromatography, recrystallized by methanol and DCM.

Yield: 50%, Light green, **m.p.** 212 – 215 ^{o}C.

^{1}H NMR ($CDCl_3$, 400 MHz, δ with TMS = 0); 3.07 (1H, dd, J = 4 Hz), 3.98 (1H, t, J_{23} = 12 Hz), 5.64 (1H, dd, J = 4 Hz), 6.61 (1H, d, J = 8 Hz), 6.84 (1H, d, J = 8 Hz), 6.93 (1H, t, J = 8 Hz), 7.31 (1H, s), 7.41 (3H, t, J = 4 Hz), 7.50 (2H, d, J = 4 Hz), 7.63 (2H, d, J = 4 Hz), 7.80 (1H, s), 7.92 (1H,d, J= 8 Hz).

Mass (EI): Calculated for $C_{24}H_{16}Br_2ClN_3$: 538.94 $[M]^{+}$; found 538, [M+2] peak at 541.

5.2.4 *In silico* study of the synthesized compounds

5.2.4.1: Materials and Methods

Mac Operating System platform installed on Apple I Mac was used to perform docking studies on Maestro 11.1 (Schrodinger 2017). The study was done to identify the possible binding modes of the selected ligands to the active site of the receptor.

5.2.4.2 Selection and preparation of ligands

Ligand preparation was done by using the application Ligrep wizard of Maestro 11.1 (Schrodinger 2017). In this step, ligand structure was converted into a 3D form, from 2D, hydrogen atoms were added, discrepancies between bond lengths and angle were resolved, low energy structure and ring conformation followed by minimization and OPLS 2005 force field were conducted for the preparation of data. Consecutively, the rest of the factors such as ionization state were not altered, and specified chirality was retained.

5.2.4.3 Preparation of the Protein Molecules

The PDB for the X-ray crystallographic structure of reverse transcriptase (PDB ID: 4I2P) prepared by Maestro 11.1 protein preparation wizard was obtained from the Protein Data Bank (RSCB). Protein preparation was done in the protein preparation wizard of Schrodinger maestro software. Following steps were done to prepare protein:

- Assignment of bond orders.
- Additions of hydrogen atoms.
- Deletion of the bonds to metal.
- Setting of the formal charge on the metal.
- Deletion of the neighboring atoms that were at a distance more than 5Å.
- The addition of any missing disulphide bonds was done.
- Optimization of hydrogen bonds was done at pH 7.0.
- Overlapping issues in the hydrogen bond network were solved by reorienting hydroxyl group, water molecules, and amino acids.
- In the tab “Review and modify”, only the required part of the protein under study is kept by making a selection and the rest was deleted.
- Then, possible protonation states of the co-crystallized ligand were generated by clicking on generate states option. The structure of the ligand was reviewed to solve the problems, if any.
- Finally, with the help of restrained minimization, refinement of the structure was done.

5.2.4.4 Receptor Grid Generation

Ligand binded within the X-ray crystal structure of a protein was utilized by Glide molecular docking for the identification of active site receptor grid. Thus, the ligands were assisted by grid based molecular docking to bind in more than one possible conformation. 0.25 Å, scaling factor and 1.0 Å, partial charge cut off of Van Der Waals radius and other parameters were also applied.

5.2.4.5 Glide Molecular Docking

After the preparation of the ligands, protein and the grid on the active site of the target protein, molecular docking was carried out. Glide molecular docking used computational simulation method for the evaluation of binding poses.

Glide systematic method is a newer approach for the quick, precise molecular docking, and its output G- score (which is an empirical scoring function), is the combination of various factors. The binding energy which includes Ligand-protein interaction energies was calculated in kcal/mol. Determination of H-bond, lipophilic interaction, π-π stacking interactions, internal energy, and RMSD (Root Mean Square Deviation) and desolvation energy was also done. XP visualiser was used for the analysis of the specific ligand-protein interactions. All of the selective ligands with the X-ray crystal structure were docked including reference compound using Glide.

5.2.4.6 Evaluation of the docking study

The docking score was obtained and the ligand-protein interaction pose was formed the basis of evaluation of the results of docking study. The compounds with highest dock score in magnitude and having good interaction profile were most active compounds against the target receptor protein.

CHAPTER 6

RESULTS AND DISCUSSION

6.1. Synthesis

We proposed the following synthetic route (Scheme 6.1) for the synthesis of target compounds. DCS-1 and substituted acetophenones were taken as starting materials for the synthesis of Chalcones. Further, pyrazolines were synthesized using substituted phenyl hydrazines. Synthesis was shown in **Figure 6.1**.

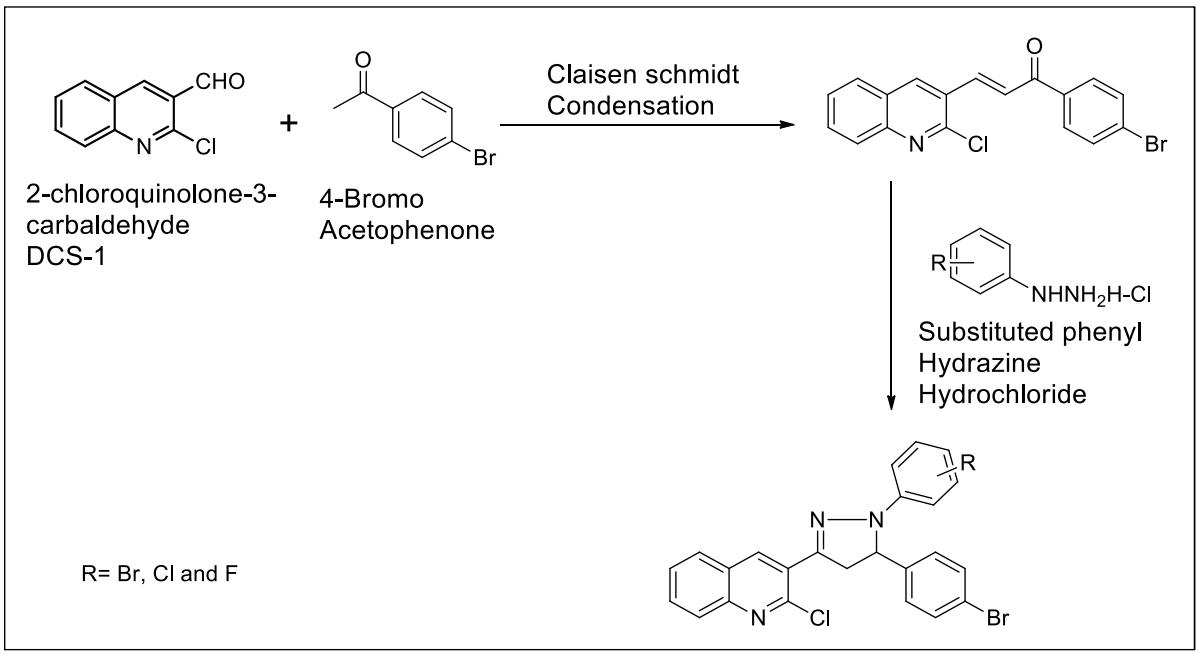

Figure 6.1 Synthetic route for the synthesis of target compounds

6.1.1 Synthesis of Chalcone:

Synthesis of chalcone was done by adding 2-Chloroquinoline-3-carbaldehyde to 4-bromoacetophenone. After adding 5ml methanol and stirred. Synthesis was shown in **Figure 6.2.**

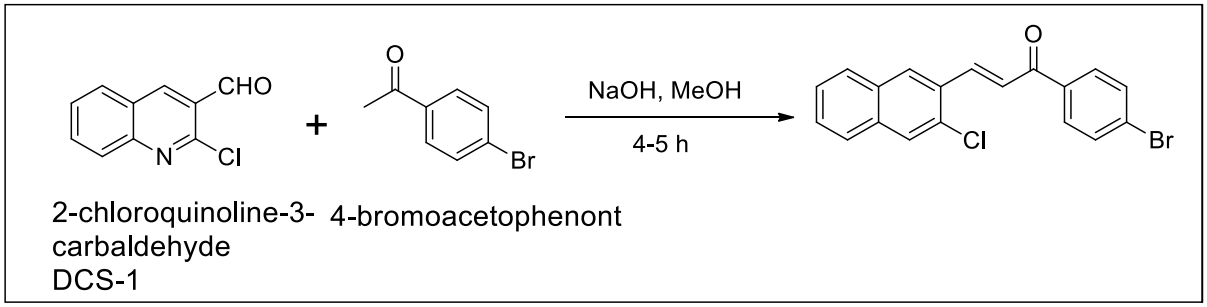

Figure 6.2 Reaction for the synthesis of chalcones

6.1.1.1 Claisen Schmidt Condensation

Mechanistically, base catalysed Claisen-Schmidt condensation is characterized by the formation of an enolate ion of the ketone. As represented in **Figure 6.3**, formation of enolate ion (Step 1) taken place as the consequences of hydrogen abstraction (alpha to the carbonyl moiety) from the ketone by the base (NaOH). This enolate ion acting as the nucleophile attacks at the electrophilic carbon of the aldehyde (Step II) in the process rendering to the electron rich which takes up the proton from aqueous solution (Step III). The final step of the reaction is dehydration (Step V) which affords synthesis of Chalcones.

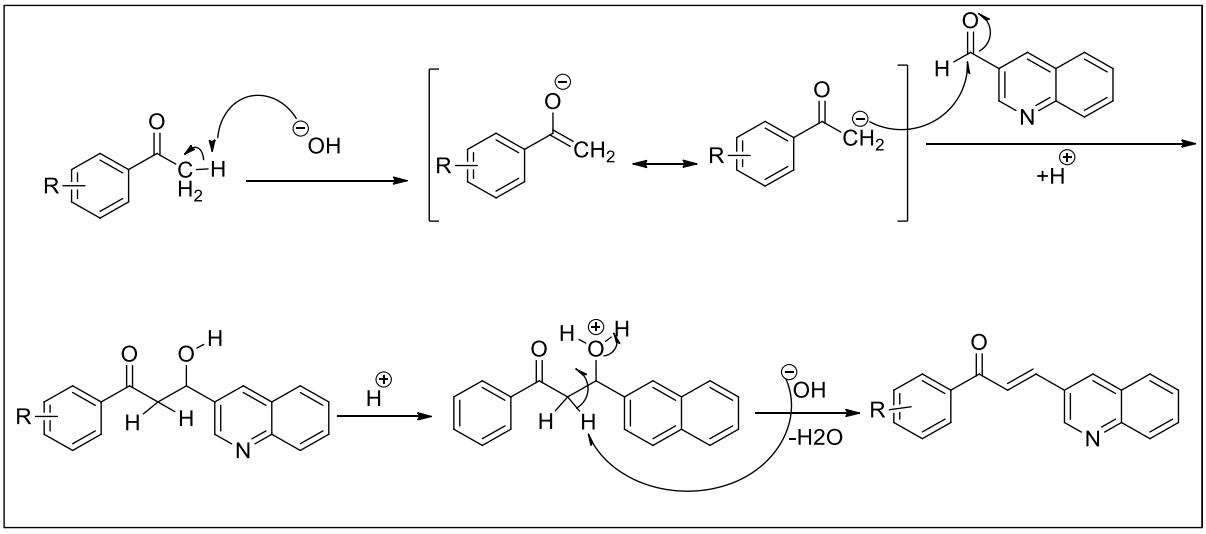

Figure 6.3 Mechanism of Claisen-Schmidt Condensation

6.1.2 Synthesis of proposed compounds

Substituted chalcone was added to substituted phenyl Hydrazine hydrochloride. After adding 5ml methanol and stirred for 4-5 h at 50^{o}C – 60^{o}C as represented in **Figure 6.4.**

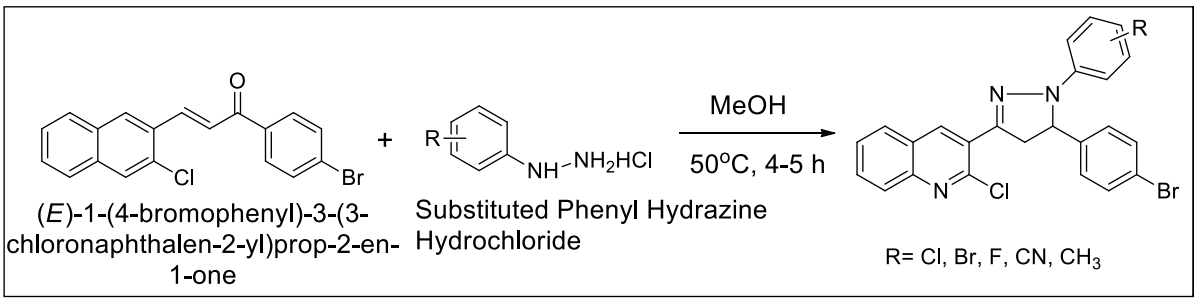

(*E*)-1-(4-bromophenyl)-3-(3-chloronaphthalen-2-yl)prop-2-en-1-one

Substituted Phenyl Hydrazine Hydrochloride

Figure 6.4 Reaction for the synthesis of proposed compounds

6.1.3 Pyrazoline synthesis

The reaction proceeds by Michael addition to the chalcones followed by proton transfer, cyclization via Claisen addition, hydrolysis and spontaneous dehydration.

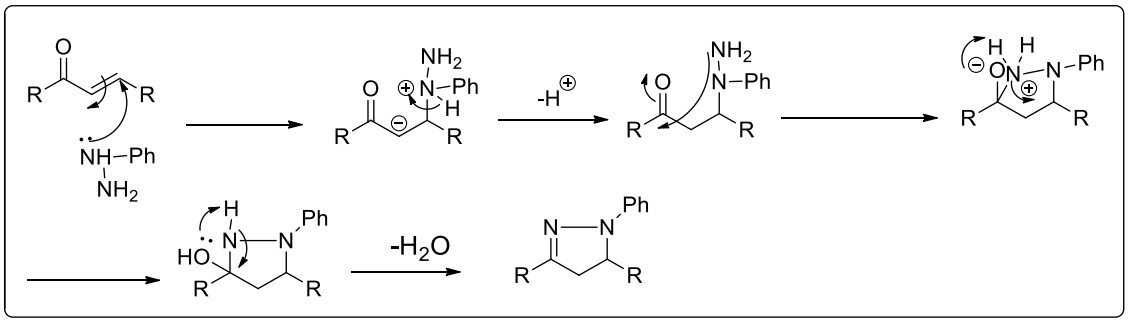

Figure 6.5 Mechanism of Pyrazoline formation

6.2 Docking studies

Docking results indicated that all the proposed ligands have a strong binding affinity for the reverse transcriptase as indicated by their docking score values that were found to be comparable with the docking score of the standard molecules elvitegravir (-8.57). Binding interactions (2D and 3D) of elvitegravir are described in **Table 6.1** and **Figure 6.6 and in figure 6.7** respectively. Compound DC-1 and DC-6 shows pi-pi interactions with Tryptophan and Tyrosine.

Table6.1. 2-D Docking pose of the synthesized compounds and their docking score

Ligands	Docking Pose	Docking score(Kcal/mole)
DC-1	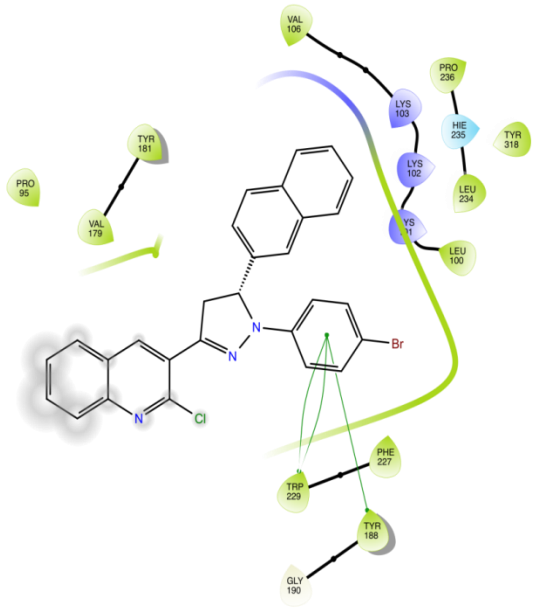	-9.34

DC-6	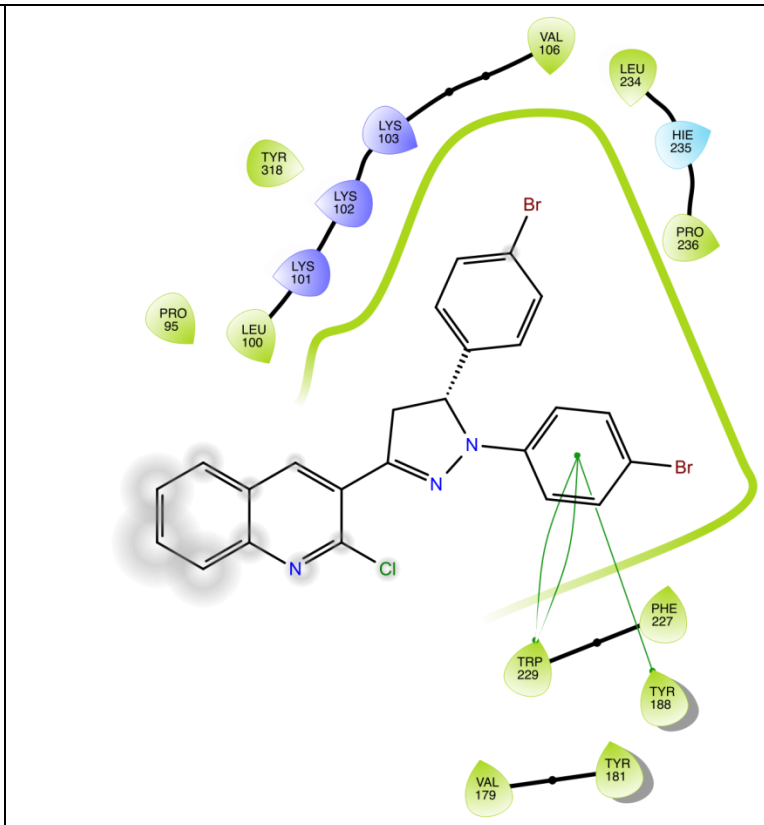	-8.76
Elvitegravir (Standard)	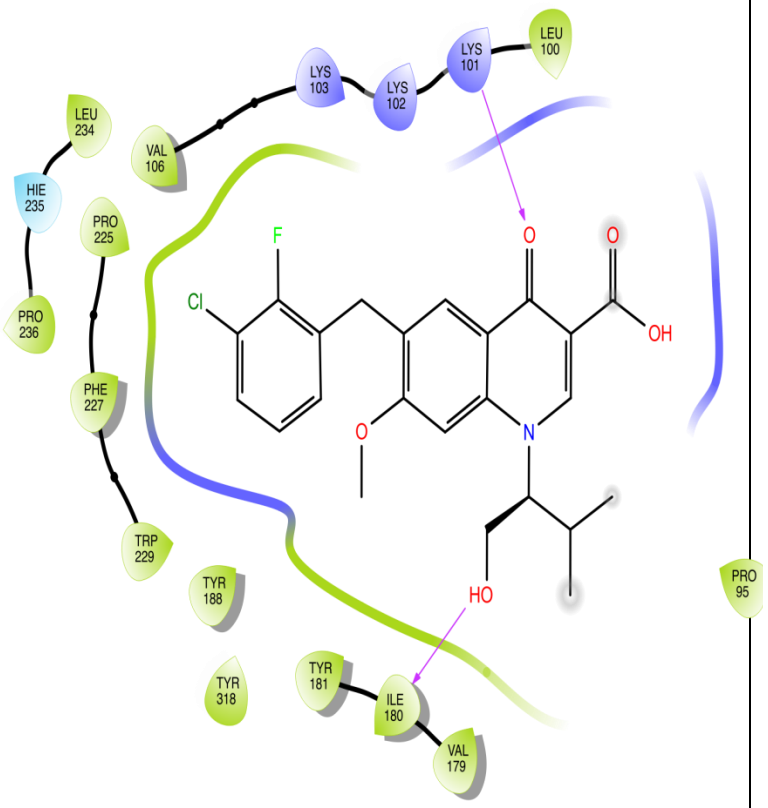	-8.57

DC-5	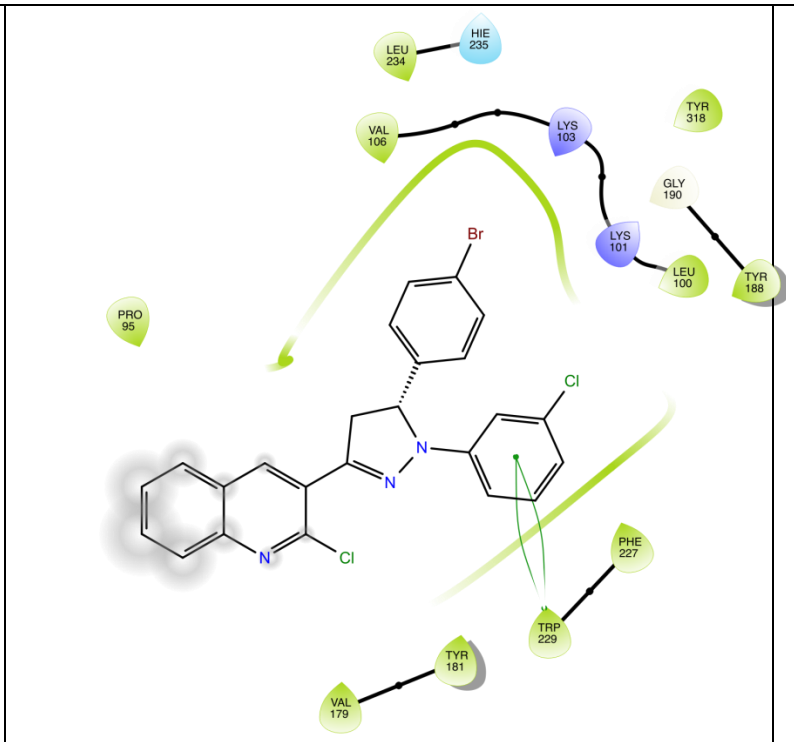	-7.93
DC-4	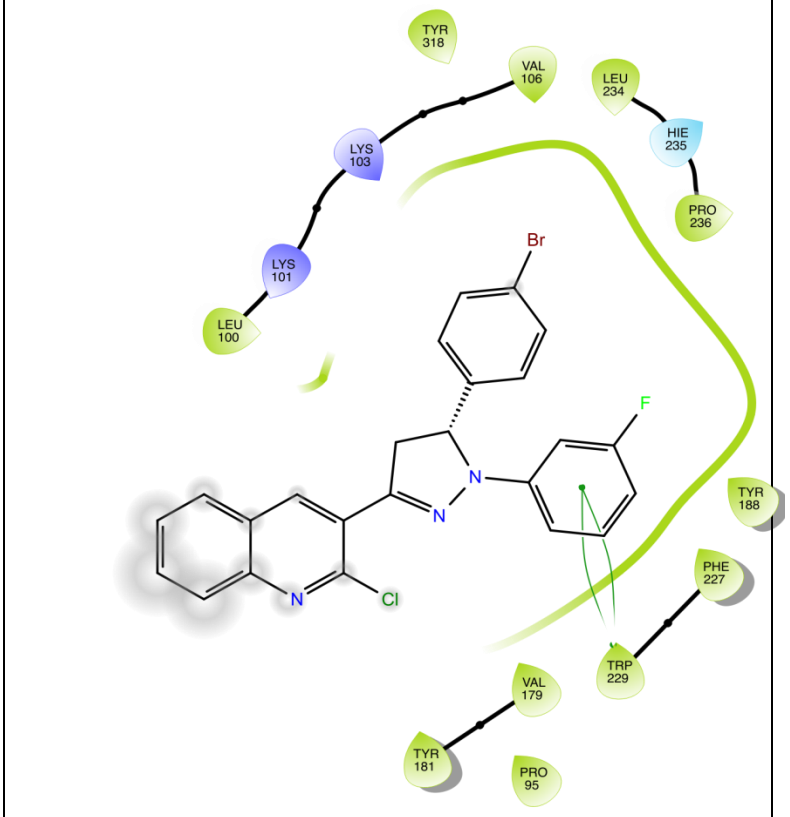	-7.75

DC-10	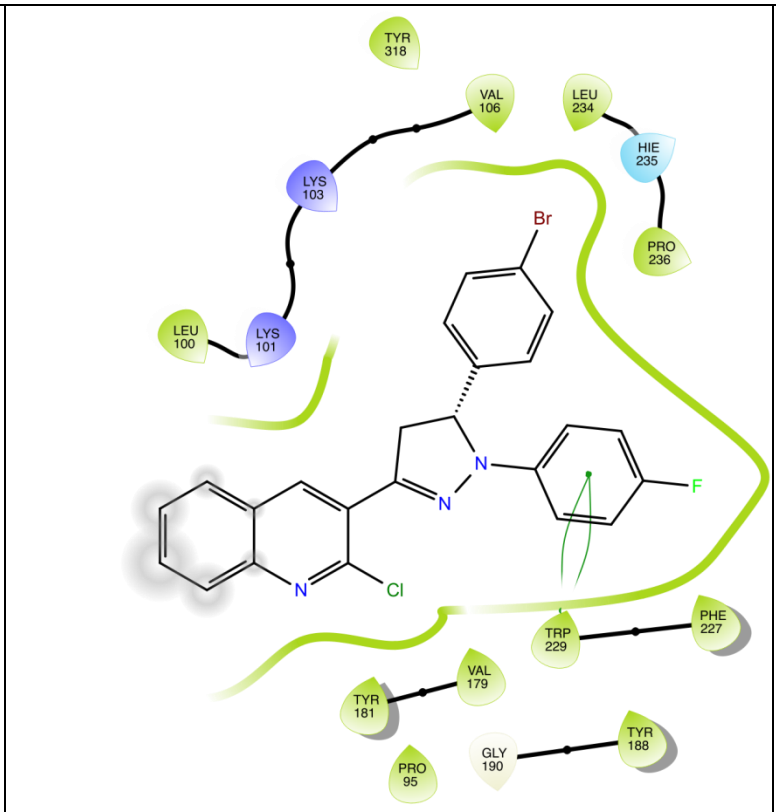	-8.51
DC-11	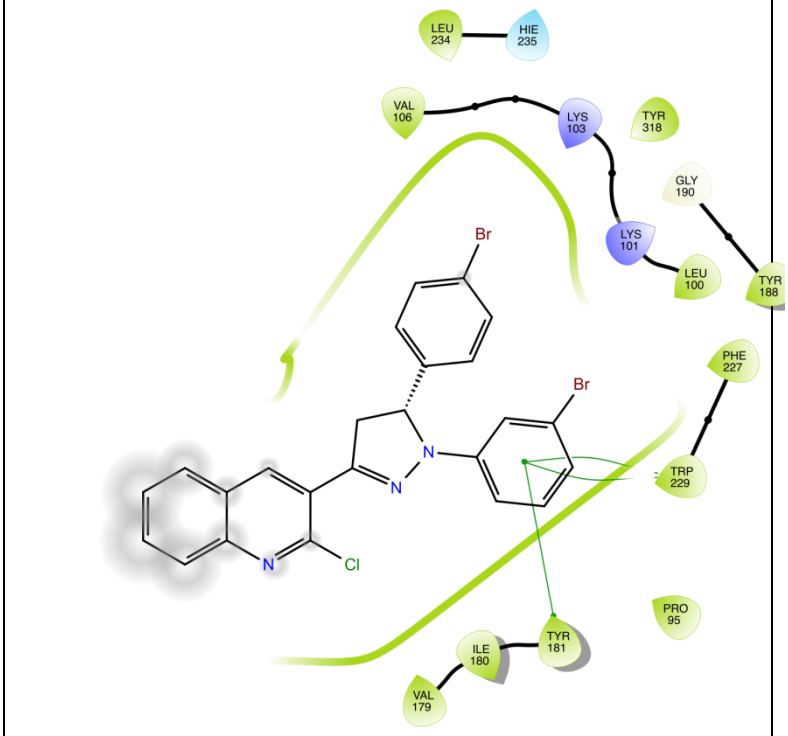	-8.08

a) Docking studies of standard inhibitor elvitegravir

Docking of standard molecule elvitegravir revealed that the standard inhibitor was having various interactions with different amino acids of the selected protein. These interactions included:

1. Hydrogen bond interaction of OH group with ILE-180.
2. Hydrogen bond interaction of O group with LYS-101.
3. The docking score of -8.57 was obtained for standard inhibitor elvitegravir.

b) Docking studies of DC-1:

Among all the docked molecules compound DC-1 was found to have best affinity as its dock score maximum i.e. -9.34.

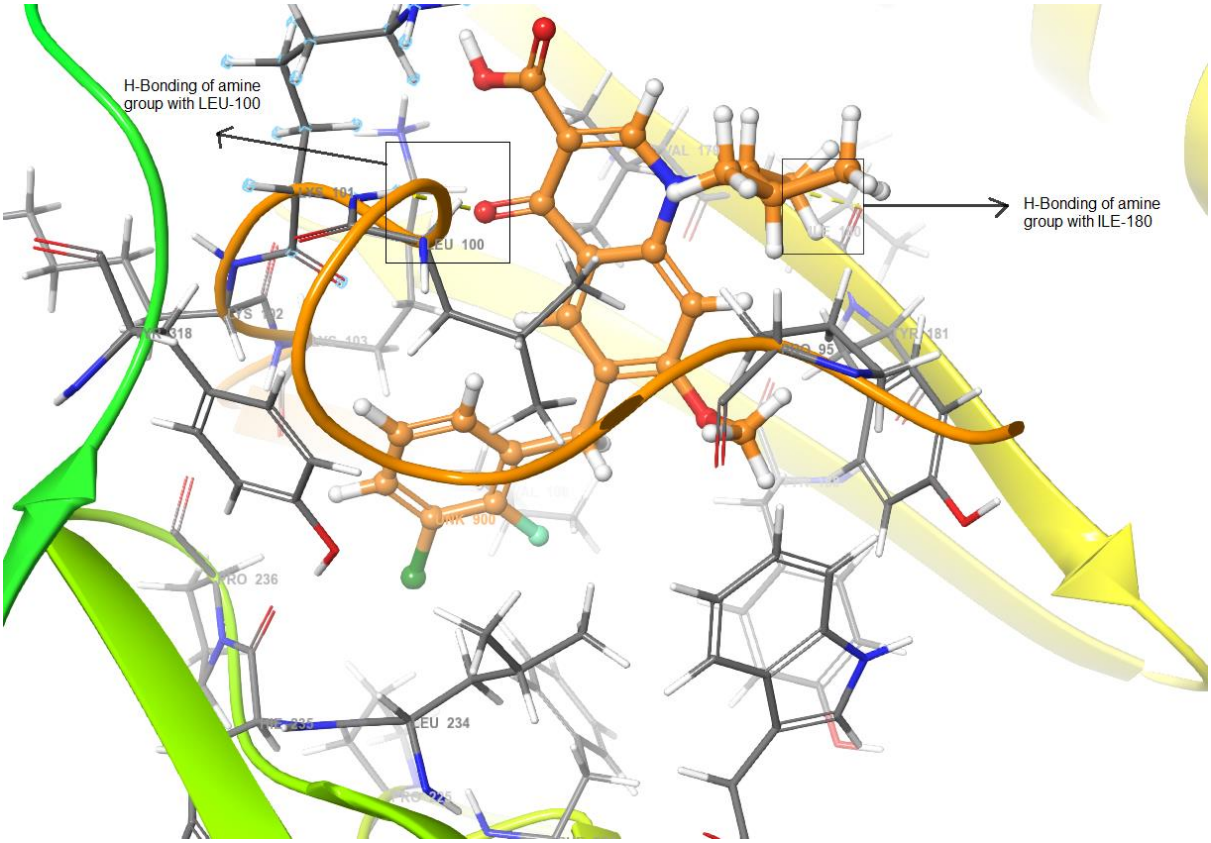

Figure 6.6 3D inteaction pattern of elvitegravir with reverse transcriptase protein (4I2P)

Table 6.1 and figure 6.7 shows the 2-D and 3-D interaction diagrams for the compound respectively.

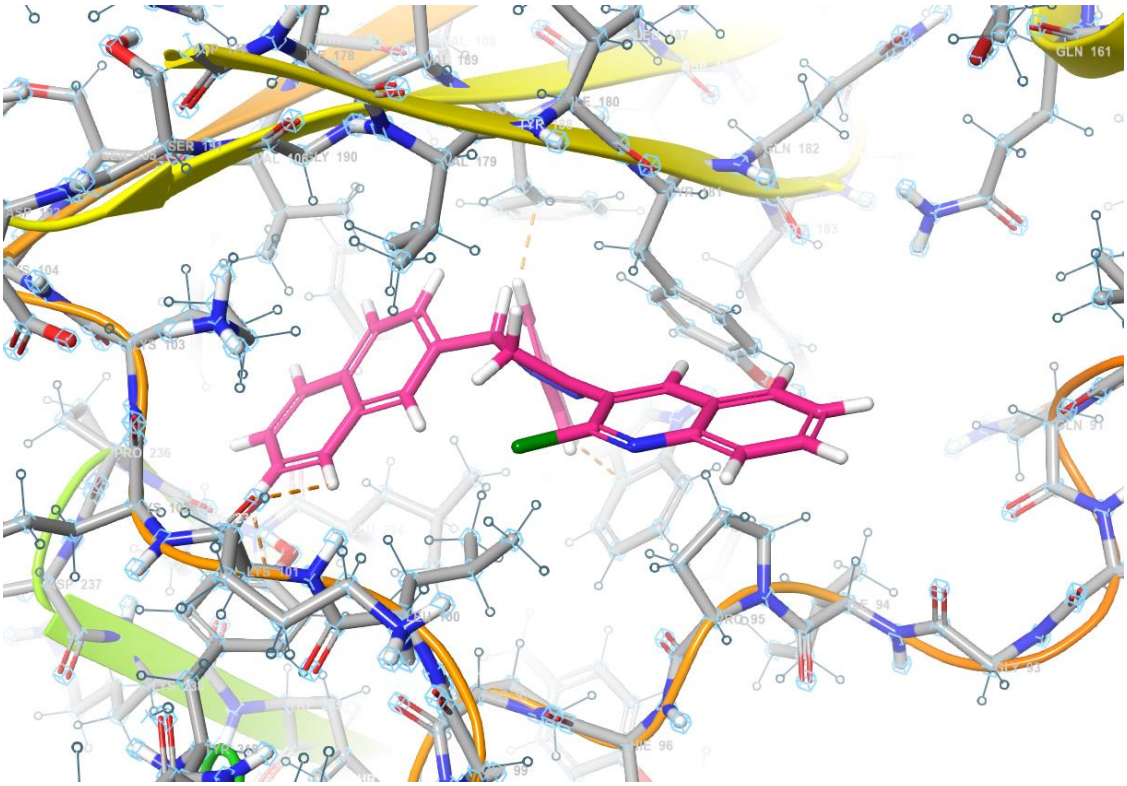

Figure 6.7 3D interaction pattern of DC-1 with RT (4I2P)

Docking of standard molecule DC-1 revealed that the standard inhibitor was having various interactions with different amino acid of the selected protein. These interactions included:

1. Pi-Pi interaction with TRP-229.
2. Pi-Pi interaction with TYR-188.

6.3 Structure activity relationship (SAR) of synthesized compounds on the basis of docking studies

1. Synthesized molecules contain 2 sites of substitution i.e. R_1 and R_2. On the basis of results of docking studies following SAR may be established and shown in **Figure 7.8**:
2. The quinoline moiety of the synthesized compounds fits in the empty cavity of the protein which increases the activity.
3. On the basis of docking score we can say that the replacement of R_1 by any electron withdrawing group or atom results in better activity.
4. The electron withdrawing group at R_2 position does not show any better affinity.

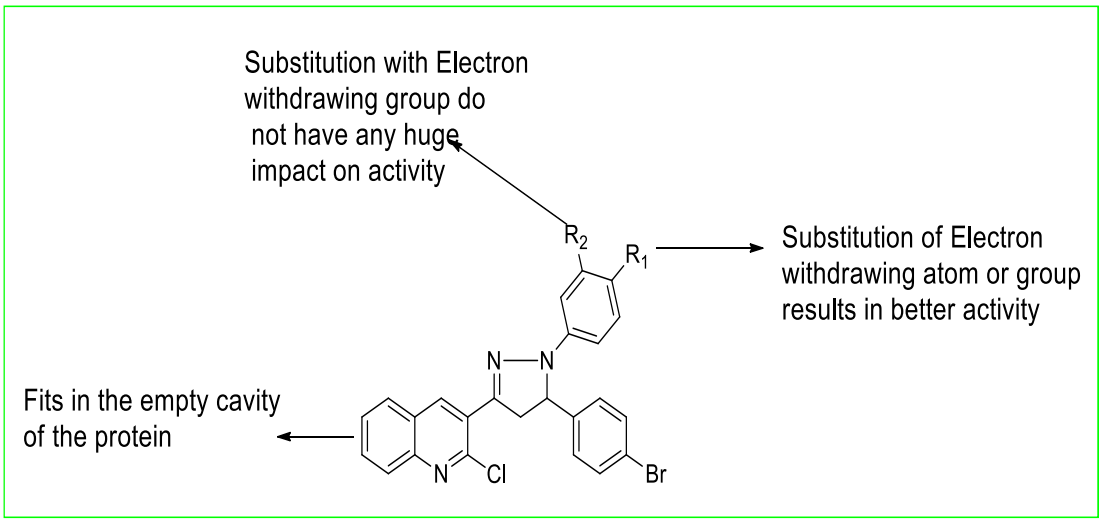

Figure 6.8 SAR of synthesized compounds

CHAPTER 7

Conclusion

7.0 Conclusion:

The proposed compounds were designed by keeping in view the structures of Elvitegravir which is FDA approved anti-HIV drug. Synthesis of designed compounds was done via chalcones and characterized by physicochemical as well as spectral means. In silico studies were performed on the 6 synthesized compounds for their HIV reverse transcriptase inhibitory activity by taking Elvitegravir as standard drug and promising results were obtained. Compound DC-1 was found to have highest affinity towards the reverse transcriptase protein (Dock score = -9.34). SAR on the basis of docking results revealed that electron withdrawing substituent on R1 position will improve the activity but on R2 position does not show much better activity.

REFERENCES

References:

Alam, C., Whyte-Allman, S. K., Omeragic, A., & Bendayan, R. (2016). Role and modulation of drug transporters in HIV-1 therapy. Advanced Drug Delivery Reviews, ***103***(Supplement C), 121-143.

Anitha, H., Sreenivasa, S., Mohan, N., Chandramohan, V., & Shivaraja, G. (2017). Journal of Applicable Chemistry. Journal of Applicable Chemistry, ***6***(1), 30-40.

Barrientos, J., Gomez, F., & Cardenas, M. (2017). Relation Between HIV Status, Risky Sexual Behavior, and Mental Health in a Gay Men Sample From Three Chilean Cities. The Journal of Sexual Medicine, ***14***(5), e263.

Best, B. M., Capparelli, E., & Stek, A. (2017). Elvitegravir/cobicistat pharmacokinetics in pregnancy and postpartum. Paper presented at the Poster presented at: Conference on Retroviruses and Opportunistic Infections,13-16

Beyhan, N., Kocyigit-Kaymakcioglu, B., Gümrü, S., & Aricioglu, F. (2017). Synthesis and anticonvulsant activity of some 2-pyrazolines derived from chalcones. Arabian Journal of Chemistry, ***10***, S2073-S2081.

Boone, M. R., Cook, S. H., & Wilson, P. A. (2016). Sexual identity and HIV status influence the relationship between internalized stigma and psychological distress in black gay and bisexual men. AIDS care, ***28***(6), 764-770.

Cai, Y., Liu, H., & Chen, H. (2018). Allosteric mechanism of quinoline inhibitors for HIV RT-associated RN ase with MD simulation and dynamics fluctuation network. Chemical Biology & Drug Design, ***91***(3), 805-816.

Chesna, L. K., & Fellner, C. (2017). Promising HIV Treatments in Late-Stage Clinical Development. Pharmacy and Therapeutics, ***42***(10), 647-649.

Das, K., Balzarini, J., Miller, M. T., Maguire, A. R., DeStefano, J. J., & Arnold, E. (2016). Conformational States of HIV-1 Reverse Transcriptase for Nucleotide Incorporation vs Pyrophosphorolysis- Binding of Foscarnet. ACS Chemical Biology, ***11***(8), 2158-2164.

Faure, C., Paques, M., & Audo, I. (2017). Electrophysiological features and multimodal imaging in ritonavir-related maculopathy. Documenta Ophthalmologica, ***135***(3), 241-248.

Gangarapu, K., Thumma, G., Manda, S., Jallapally, A., Jarapula, R., & Rekulapally, S. (2017). Design, synthesis and molecular docking of novel

structural hybrids of substituted isatin based pyrazoline and thiadiazoline as antitumor agents. Medicinal Chemistry Research, ***26***(4), 819-829.

George, A., Gopi Krishna Reddy, A., Satyanarayana, G., & Raghavendra, N. K. (2018). 1, 2, 3, 4-Tetrahydroisoquinolines as inhibitors of HIV-1 integrase and human LEDGF/p75 interaction. Chemical Biology & Drug Design, **91**,1133-1140

Ghosh, S., Mondal, L., Chakraborty, S., & Mukherjee, B. (2017). Early Stage HIV Management and Reduction of Stavudine-Induced Hepatotoxicity in Rats by Experimentally Developed Biodegradable Nanoparticles. AAPS PharmSciTech, ***18***(3), 697-709.

Gupta, S. K., & Mishra, A. (2016). Synthesis of novel Thiazolidinones substituted Quinoline derivatives as potent Anti-inflammatory and Analgesic agents. Advances in Bioresearch, ***7***(5),154-161.

Ikuma, M., Watanabe, D., Yagura, H., Ashida, M., Takahashi, M., Shibata, M., .Sugiura, W. (2016). Therapeutic Drug Monitoring of Anti-human Immunodeficiency Virus Drugs in a Patient with Short Bowel Syndrome. Internal Medicine, ***55***(20), 3059-3063.

Kassutto, S., & Rosenberg, E. S. (2004). Primary HIV Type 1 Infection. Clinical Infectious Diseases, ***38***(10), 1447-1453.

Kedjadja, A., Bouraiou, A., & Merdes, R. (2018). Synthesis and Spectral Characterization of Novel 2-Pyrazoline and Bis-2-Pyrazoline Containing Quinoline Moiety. International Journal of Organic Chemistry, ***8***(01), 105-114.

Kirchhoff, F. (2013). HIV Life Cycle: Overview. Encyclopedia of AIDS, 1-9.

Kohlstaedt, L., Wang, J., Friedman, J., Rice, P., & Steitz, T. (1992). Crystal structure at 3.5 A resolution of HIV-1 reverse transcriptase complexed with an inhibitor. Science, ***256***(5065), 1783-1790.

Kwon, Y. S., Park, S. H., Kim, M.-A., Kim, H. J., Park, J. S., Lee, M. Y., Carossino, M. (2017). Risk of mortality associated with respiratory syncytial virus and influenza infection in adults.Viral diseases. BMC Infectious Diseases, ***17***(1), 785,2-9.

Lee, H. Y., Nepali, K., Huang, F. I., Chang, C. Y., Lai, M. J., Li, Y. H., Liou, J. P. (2018). (N-Hydroxycarbonylbenylamino) quinolines as selective histone deacetylase 6 inhibitors suppress growth of multiple myeloma in vitro and in vivo. Journal of Medicinal Chemistry, ***61***(3), 905-917.

Liu, X. H., Fang, Y. M., Xie, F., Zhang, R. R., Shen, Z. H., Tan, C. X., Huang, H. Y. (2017). Synthesis and in vivo fungicidal activity of some new quinoline derivatives against rice blast. Pest Management Science, ***73***(9), 1900-1907.

Mahmoodi, N. O., Zeydi, M. M., Mamaghani, M., & Montazeri, N. (2017). Synthesis and antibacterial evaluation of several novel tripod pyrazoline with triazine core (TPTC) compounds. Research on Chemical Intermediates, ***43***(4), 2641-2651.

Mailler, E., Bernacchi, S., Marquet, R., Paillart, J.-C., Vivet-Boudou, V., & Smyth, R. P. (2016). The Life-Cycle of the HIV-1 Gag–RNA Complex. Viruses, ***8***(9), 248.

Mandala, D., Thompson, W. A., & Watts, P. (2016). Synthesis routes to anti-HIV drugs. Tetrahedron, ***72***(24), 3389-3420.

Manivannan, C., & Santhi, N. (2017). Synthesis, characterization and antifungal activity of some fluorine containing 1, 3, 5-trisubstituted pyrazoline derivatives. World News of Natural Sciences, ***10***, 86-94.

Matheron, S., Descamps, D., Gallien, S., Besseghir, A., Sellier, P., Blum, L., Sud Sida-Hiv Hépatites, H. I. V. T. S. G. (2018). Raltegravir/Emtricitabine/Tenofovir Combination in Human Immunodeficiency Virus Type 2 (HIV-2) Infection: A Phase 2, Noncomparative Trial (ANRS 159 HIV-2). Clinical Infectious Diseases 2018, ciy245-ciy245.

Melo, B. C., Bernardino, A. M., Polillo, G., Pereira, H. S., Paixão, I. C., Ribeiro, M. S., & Borges, J. C. (2017). Novel 4-arylaminoquinoline-3-carbonitriles as Inhibitors of HIV-1 Reverse Transcriptase. Journal of Heterocyclic Chemistry, ***54***(6), 3051-3055.

Miller, M. T., Tuske, S., Das, K., DeStefano, J. J., & Arnold, E. (2016a). Structure of HIV-1 reverse transcriptase bound to a novel 38-mer hairpin template-primer DNA aptamer. Protein Science, ***25***(1), 46-55.

Miller, M. T., Tuske, S., Das, K., DeStefano, J. J., & Arnold, E. (2016b). Structure of HIV-1 reverse transcriptase bound to a novel 38-mer hairpin template-primer DNA aptamer. Protein Science, ***25***(1), 46-55.

Nguyen, H. T., Madani, N., Ding, H., Elder, E., Princiotto, A., Gu, C., Sodroski, J. G. (2017). Evaluation of the contribution of the transmembrane region to the ectodomain conformation of the human immunodeficiency virus (HIV-1) envelope glycoprotein. Virology journal, ***14***(1), 2-16.

Ntshongontshi, N., Baleg, A. A. A., Ajayi, R. F., Rassie, C., Nxusani, E., Wilson, L., Douman, S. F. (2016). Cytochrome P450-3A4/Copper-Poly (Propylene Imine)-Polypyrrole Star Co-Polymer Nanobiosensor System for Delavirdine-A Non-Nucleoside Reverse Transcriptase Inhibitor HIV Drug. Paper presented at the Journal of Nano Research; pp 265-280.

Pancera, M., Changela, A., & Kwong, P. D. (2017). How HIV-1 entry mechanism and broadly neutralizing antibodies guide structure-based vaccine design. Current Opinion in HIV and AIDS, ***12***(3), 229-240.

Parekh, N., Maheria, K., Patel, P., & Rathod, M. (2011). Study on antibacterial activity for multidrug resistance stain by using phenyl pyrazolones substituted 3-amino 1H-pyrazolon (3, 4-b) quinoline derivative in vitro condition. Int. J. Pharm Tech Res, ***3***, 540-548.

Patel, J. J., Patel, A. P., & Chikhalia, K. H. (2018). Design and synthesis of some novel 7-substituted thiosemicarbazinyl-quinolines via Ullmann coupling reaction and examination of their antimicrobial activities. Research on Chemical Intermediates, ***44***(2), 813-828.

Penkalski, M. R., Felicilda-Reynaldo, R. F. D., & Patterson, K. (2017). Antiviral Medications, Part 2: HIV Antiretroviral Therapy. Medsurg Nursing, ***26***(5), 327-331.

Prevedel, L., Morocho, C., Bennett, M. V., & Eugenin, E. A. (2017). HIV-Associated Cardiovascular Disease: Role of Connexin 43. The American journal of pathology, ***187***(9), 1960-1970.

Reddy, V. K. (2017). Elimination of Mother-to-child Transmission of HIV-World Health Organization's South-East Asian Region Overview,1-72.

Rhodes, C. M., Chang, Y., Regan, S., Singer, D. E., & Triant, V. A. (2017). Human Immunodeficiency Virus (HIV) Quality Indicators Are Similar Across HIV Care Delivery Models ,***4*** (1), 1-7.

Samanta, P. N., & Das, K. K. (2017). Inhibition activities of catechol diether based non-nucleoside inhibitors against the HIV reverse transcriptase variants: Insights from molecular docking and ONIOM calculations. Journal of Molecular Graphics and Modelling, ***75***(Supplement C), 294-305.

Sarafianos, S. G., Marchand, B., Das, K., Himmel, D., Parniak, M. A., Hughes, S. H., & Arnold, E. (2009). Structure and function of HIV-1 reverse

transcriptase: molecular mechanisms of polymerization and inhibition. Journal Of Molecular Biology, ***385***(3), 693-713.

Sharaf, N. G., Brereton, A. E., Byeon, I.-J. L., Karplus, P. A., & Gronenborn, A. M. (2016). NMR structure of the HIV-1 reverse transcriptase thumb subdomain. Journal of Biomolecular NMR, ***66***(4), 273-280.

Shringare, S. N., Chavan, H. V., Bhale, P. S., Dongare, S. B., Mule, Y. B., Patil, S. B., & Bandgar, B. P. (2018). Synthesis and pharmacological evaluation of combretastatin-A4 analogs of pyrazoline and pyridine derivatives as anticancer, anti-inflammatory and antioxidant agents. Medicinal Chemistry Research, ***27***(4), 1226-1237.

Sowmya, P., Poojary, B., Revanasiddappa, B., Vijayakumar, M., Nikil, P., & Kumar, V. (2017). Novel 2-methyl-6-arylpyridines carrying active pharmacophore 4, 5-dihydro 2-pyrazolines: synthesis, antidepressant, and anti-tuberculosis evaluation. Research on Chemical Intermediates, ***43***(12), 7399-7422.

Srilakshmi, G., & Adapa, S. R. (2017). Synthesis, characterization and antiinflammatory activity of some novel quinoline derivatives,***7***(3), 661-669.

Swain, P., Das, J. K., Jha, S., & Sharnngadharan, G. K. (2017). Determinants of HIV positivity among injecting drug users in Delhi and Punjab. Indian Journal of Sexually Transmitted Diseases and AIDS, ***38***(2), 121-127.

Yamani, L. N., Yano, Y., Utsumi, T., Wasityastuti, W., Rinonce, H. T., Widasari, D. I., Hayashi, Y. (2017). Profile of Mutations in the Reverse Transcriptase and Overlapping Surface Genes of Hepatitis B Virus (HBV) in Treatment-Naïve Indonesian HBV Carriers. Japanese Journal Of Infectious Diseases, ***70***(6), 647-655.

Yusuf, M., & Jain, P. (2014). Synthetic and biological studies of pyrazolines and related heterocyclic compounds. Arabian Journal of Chemistry, ***7***(5), 553-596.

APPENDIX

9 (A): Spectral Data of the synthesized compound

DCS-1

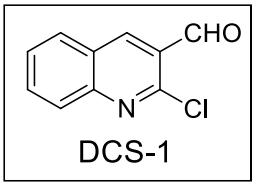

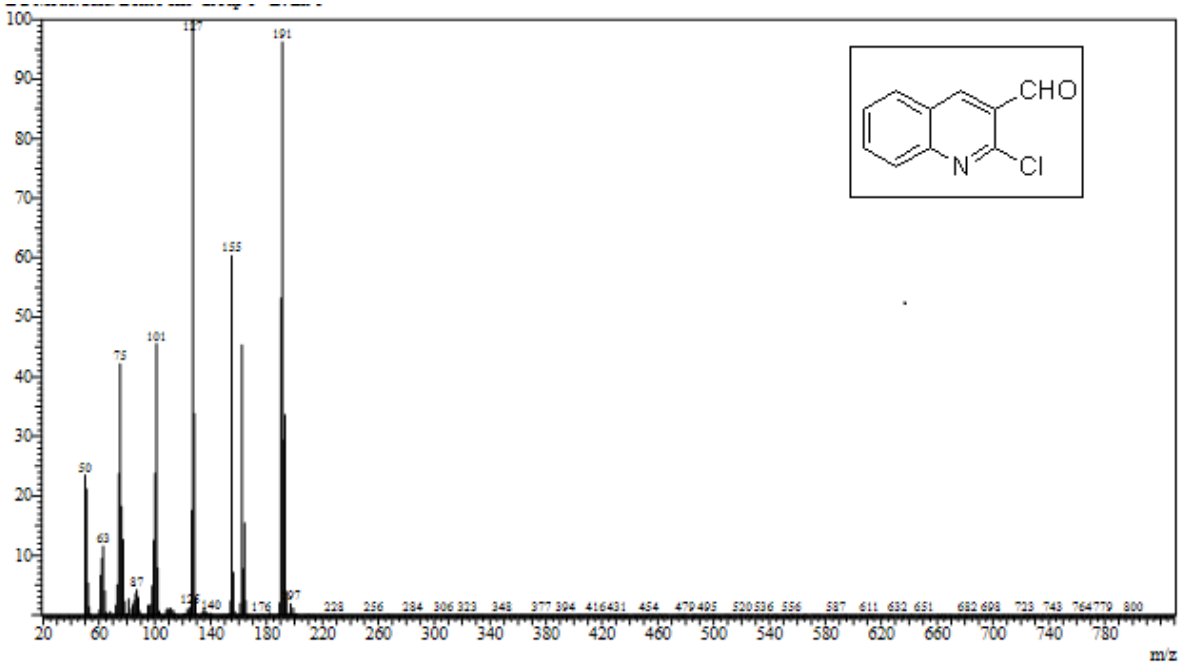

Figure 1 Mass spectrum of DCS-1

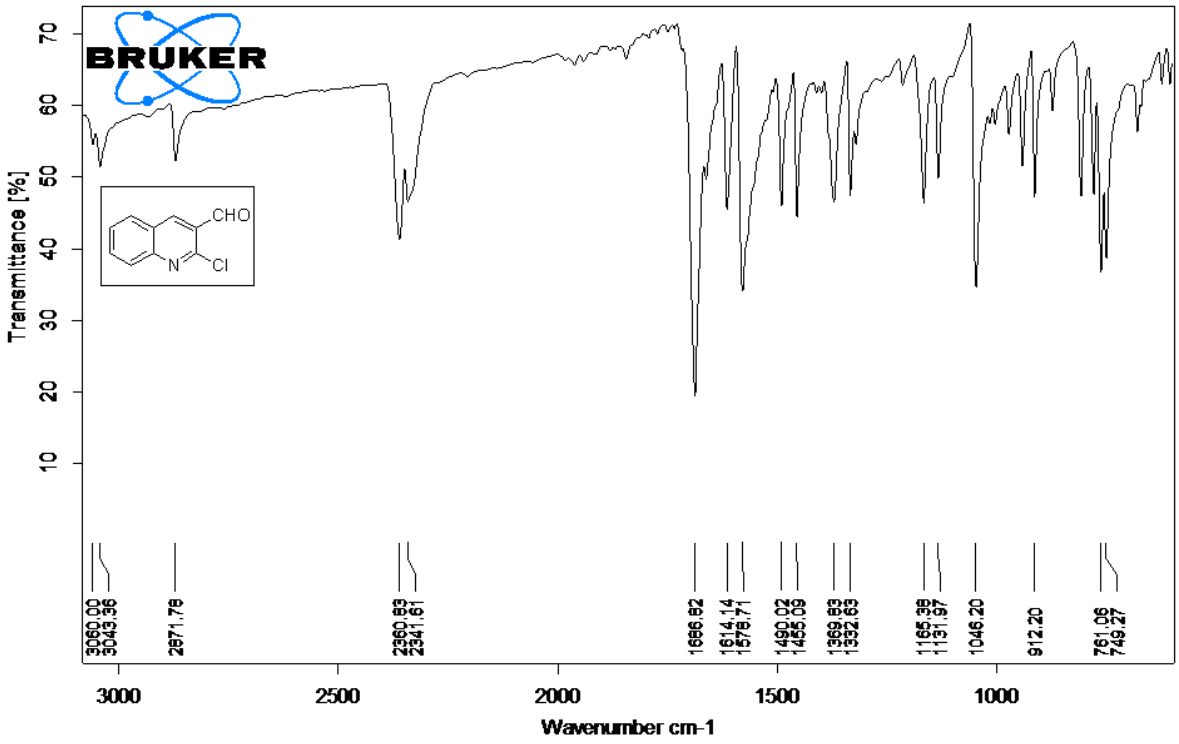

Figure 2 I.R spectrum of DCS-1

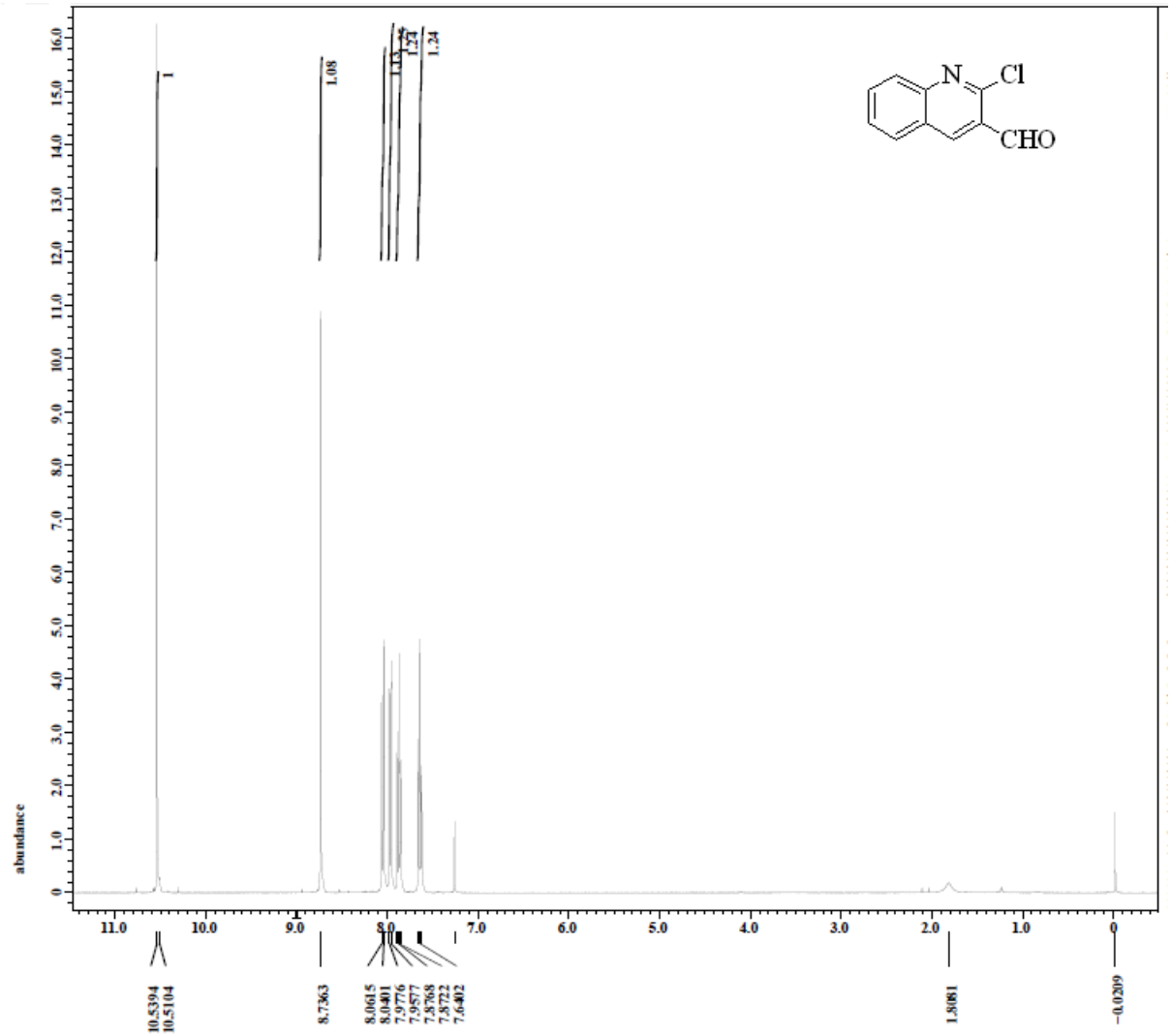

Figure 3 ^{1}H NMR spectrum of DCS-1

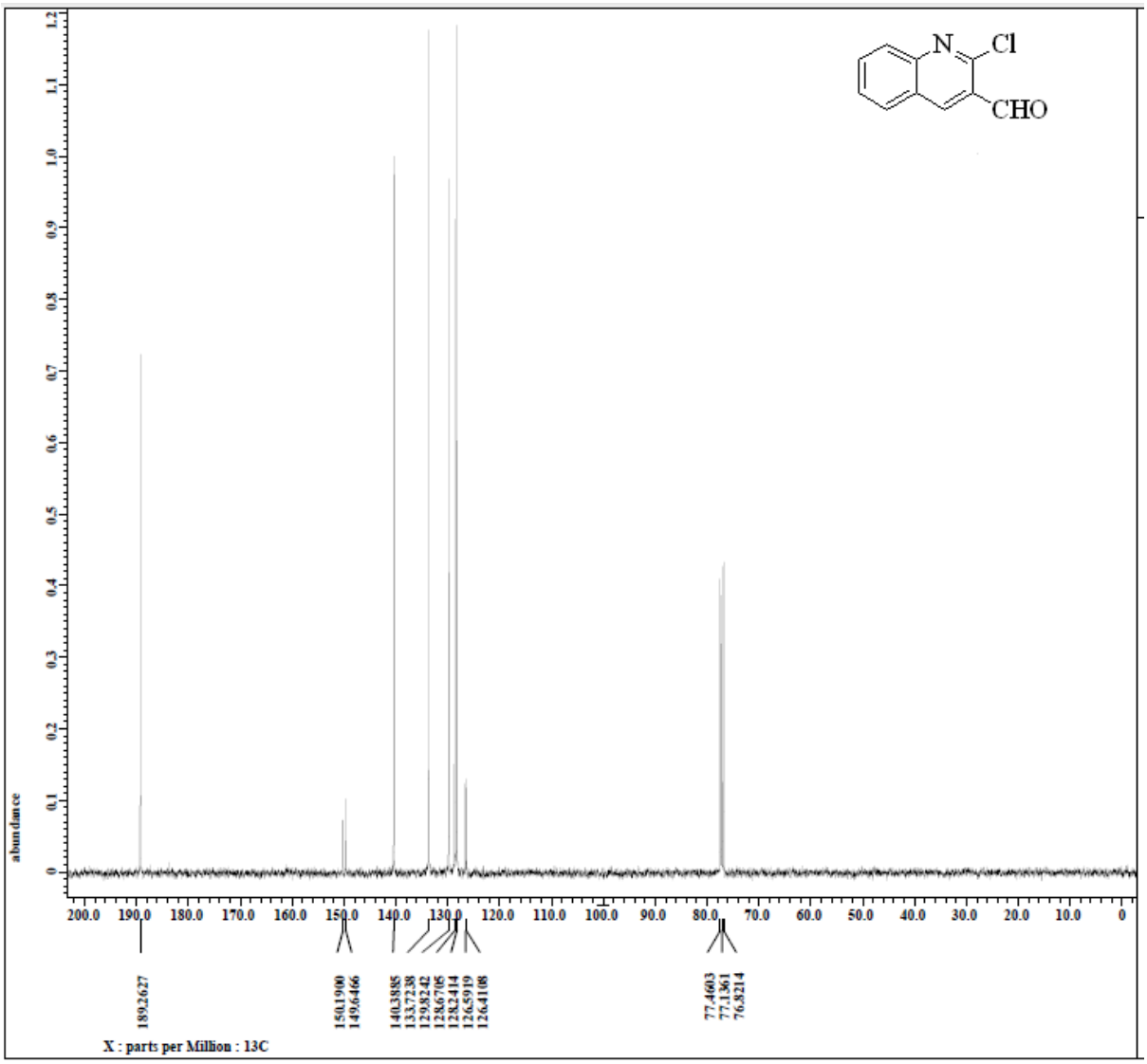

Figure 4 ^{13}CNMR spectrum of DCS-1

CHALCONES

DCC-2

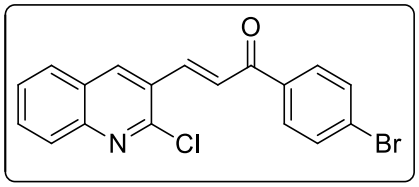

DCC-2

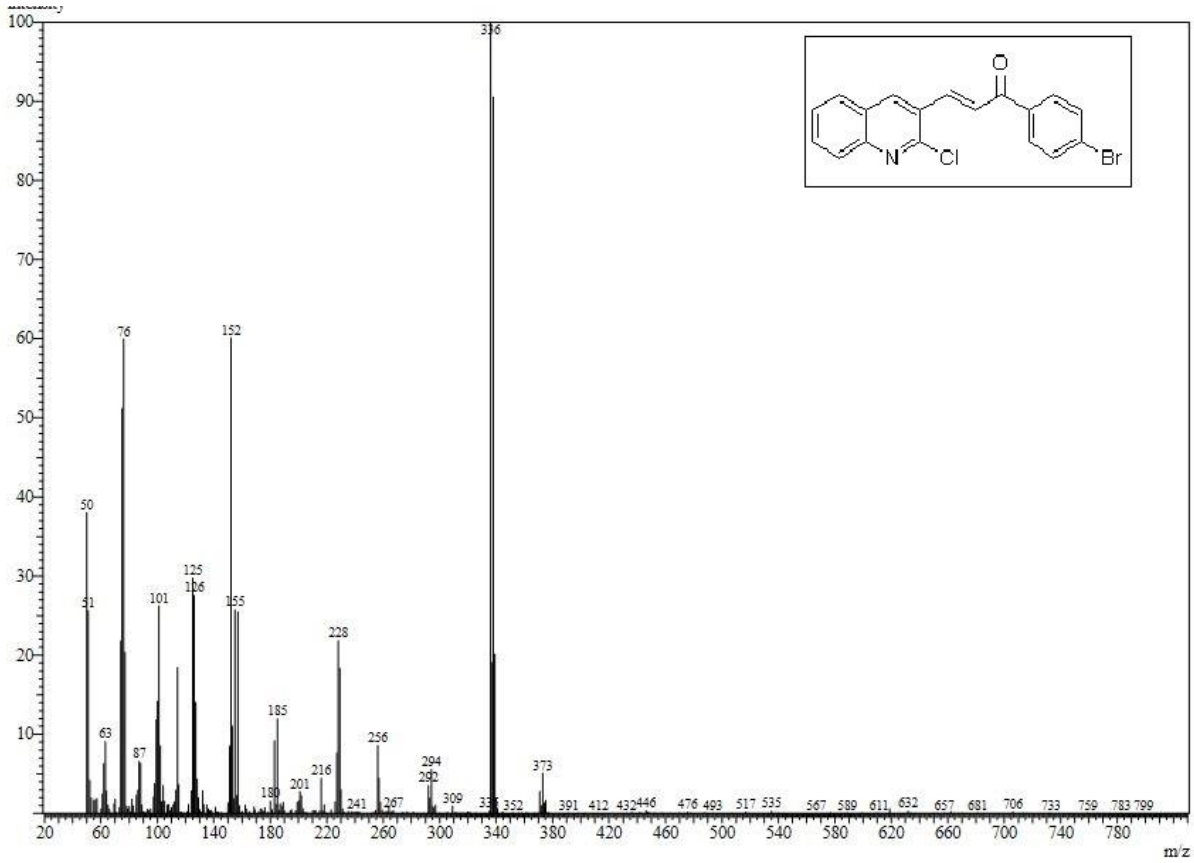

Figure 5 Mass spectrum of DCC-2

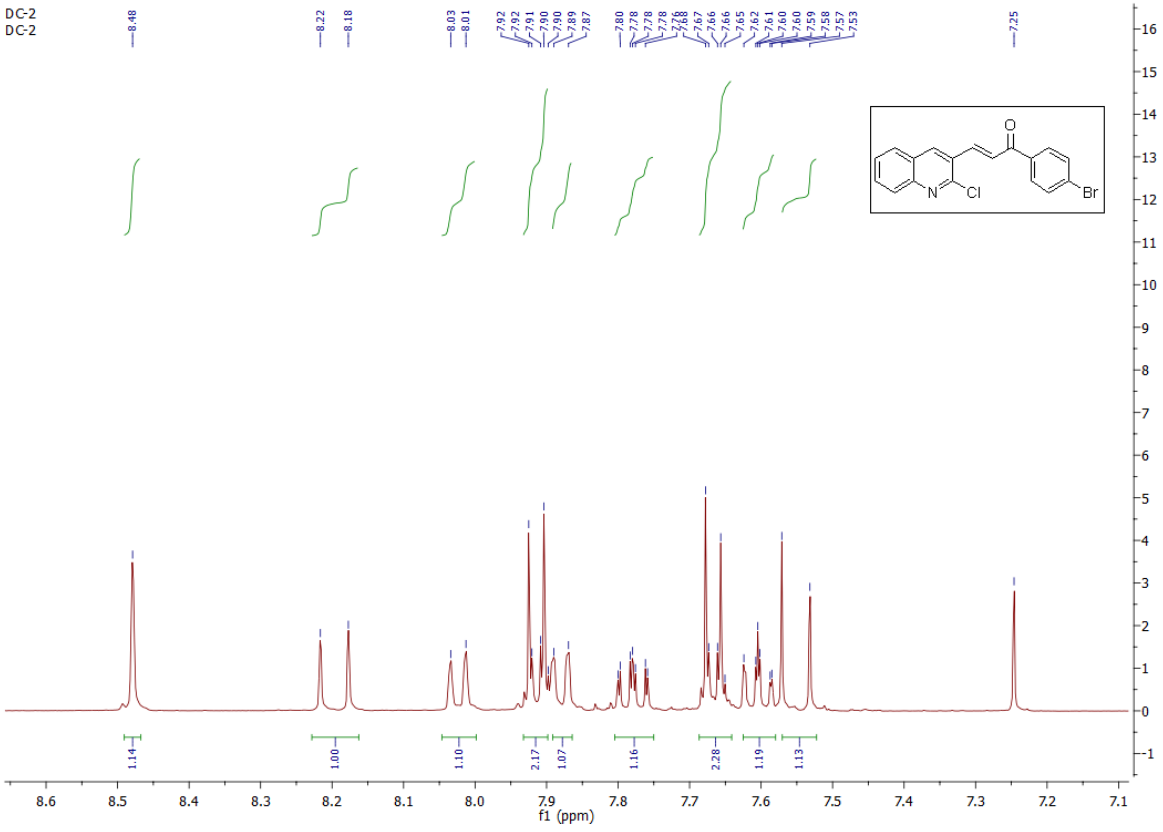

Figure 6 ^{1}H NMR spectrum of DCC-2

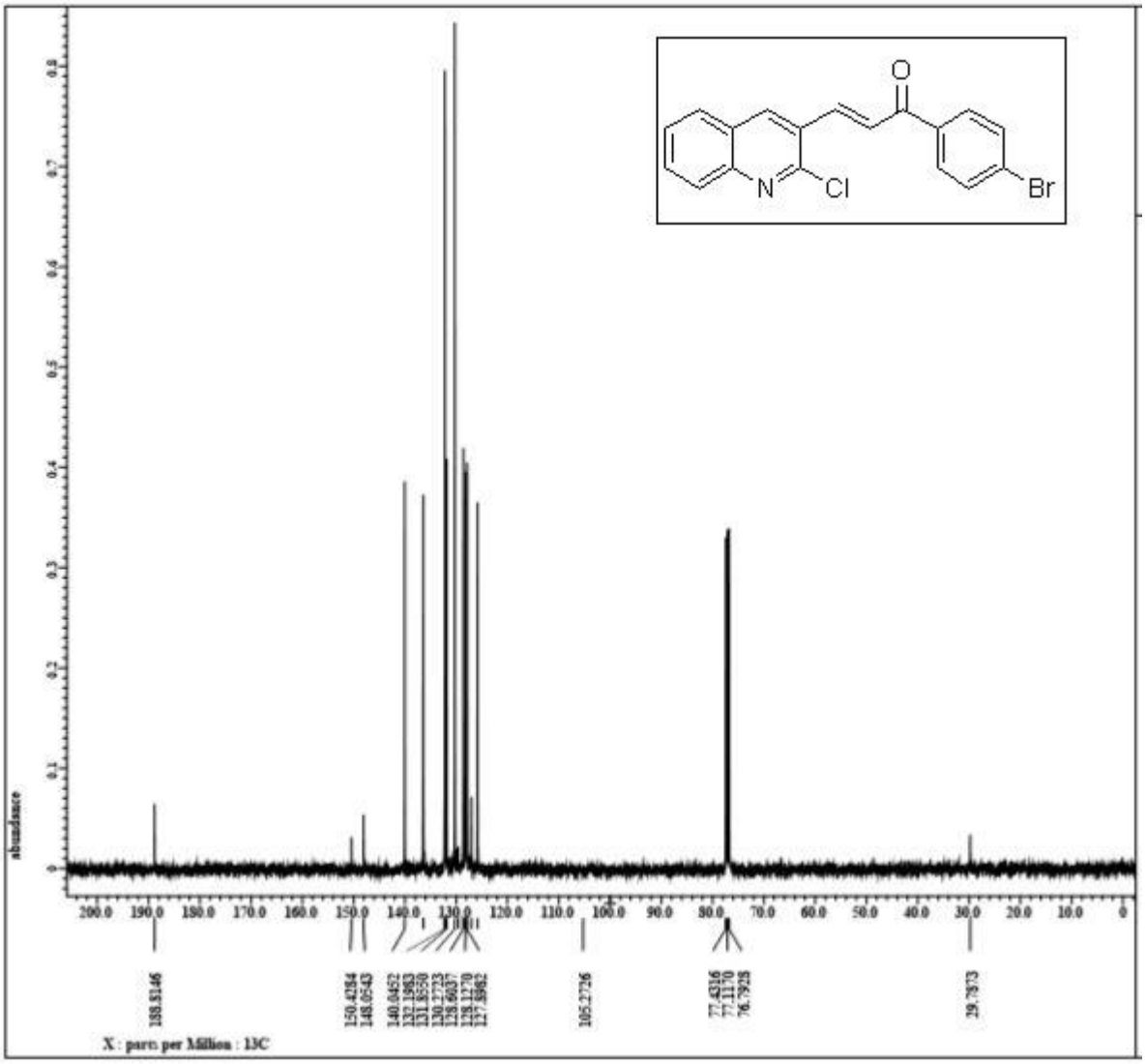

Figure 7 ^{13}C-NMR of DCC-2

FINAL COMPOUNDS

DC- 1

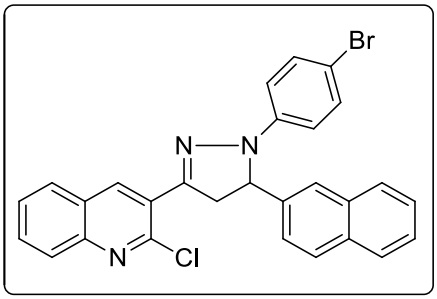

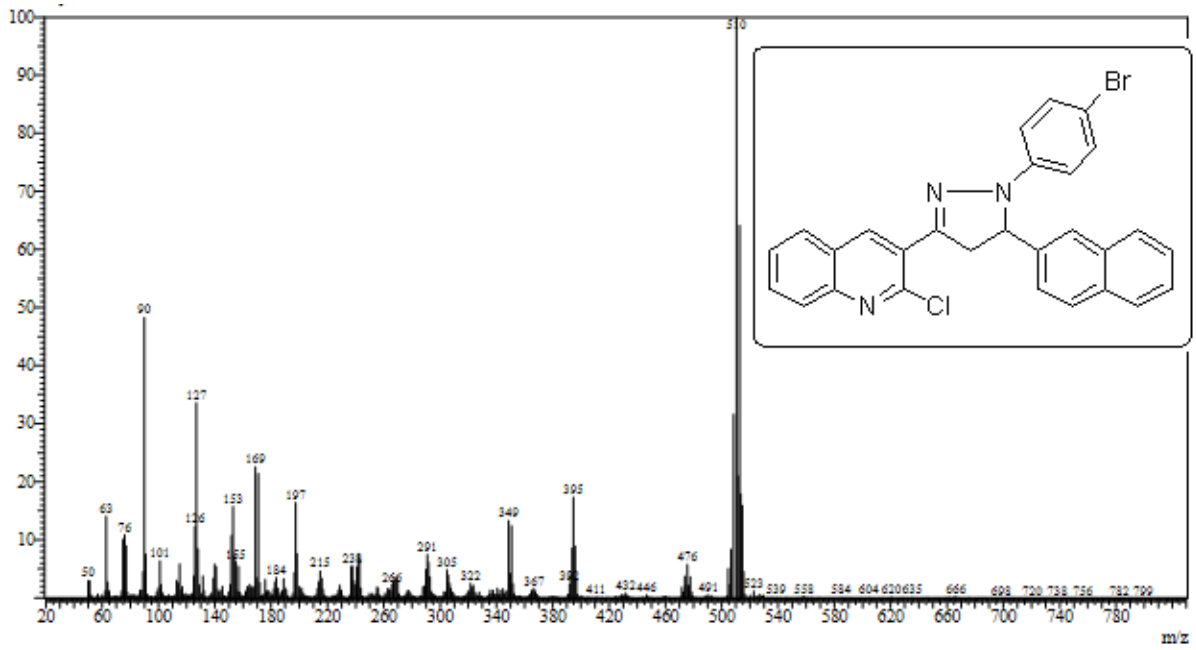

Figure 8 Mass spectrum of DC-1

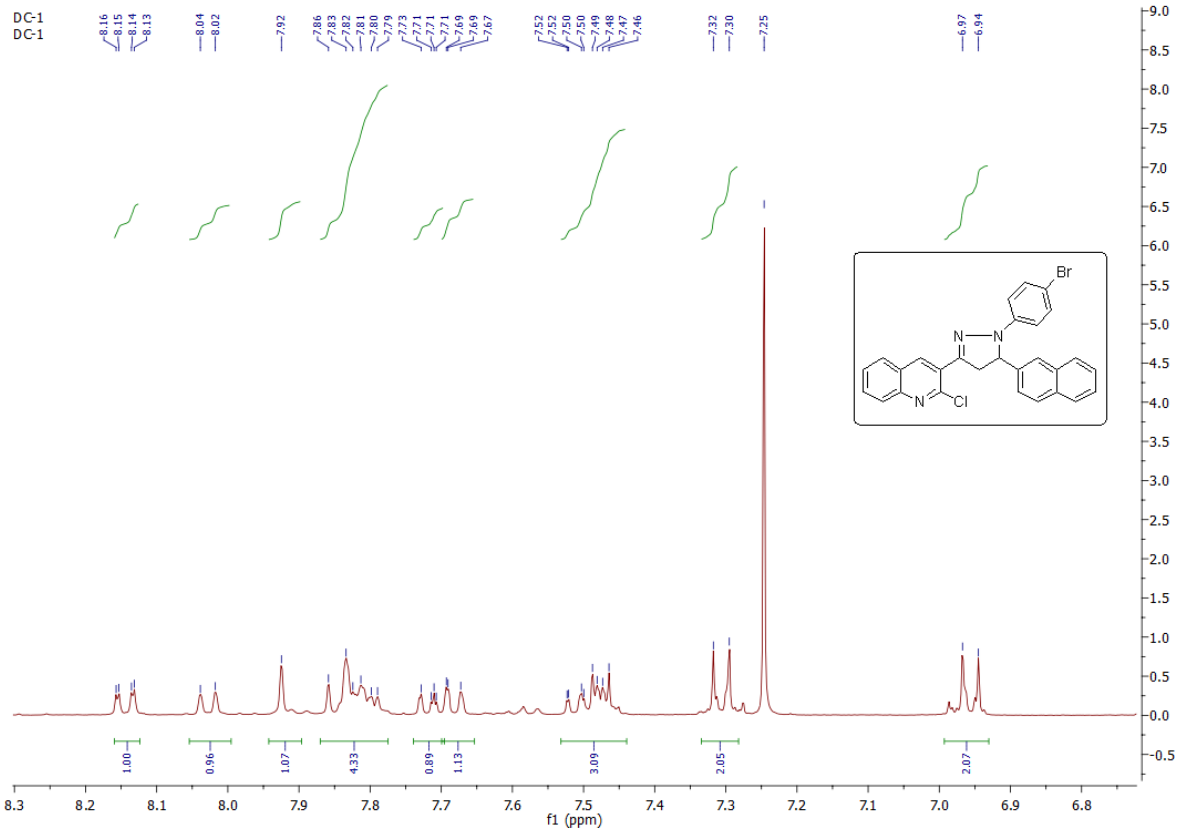

Figure 9 ^{1}H NMR spectrum of DC-1

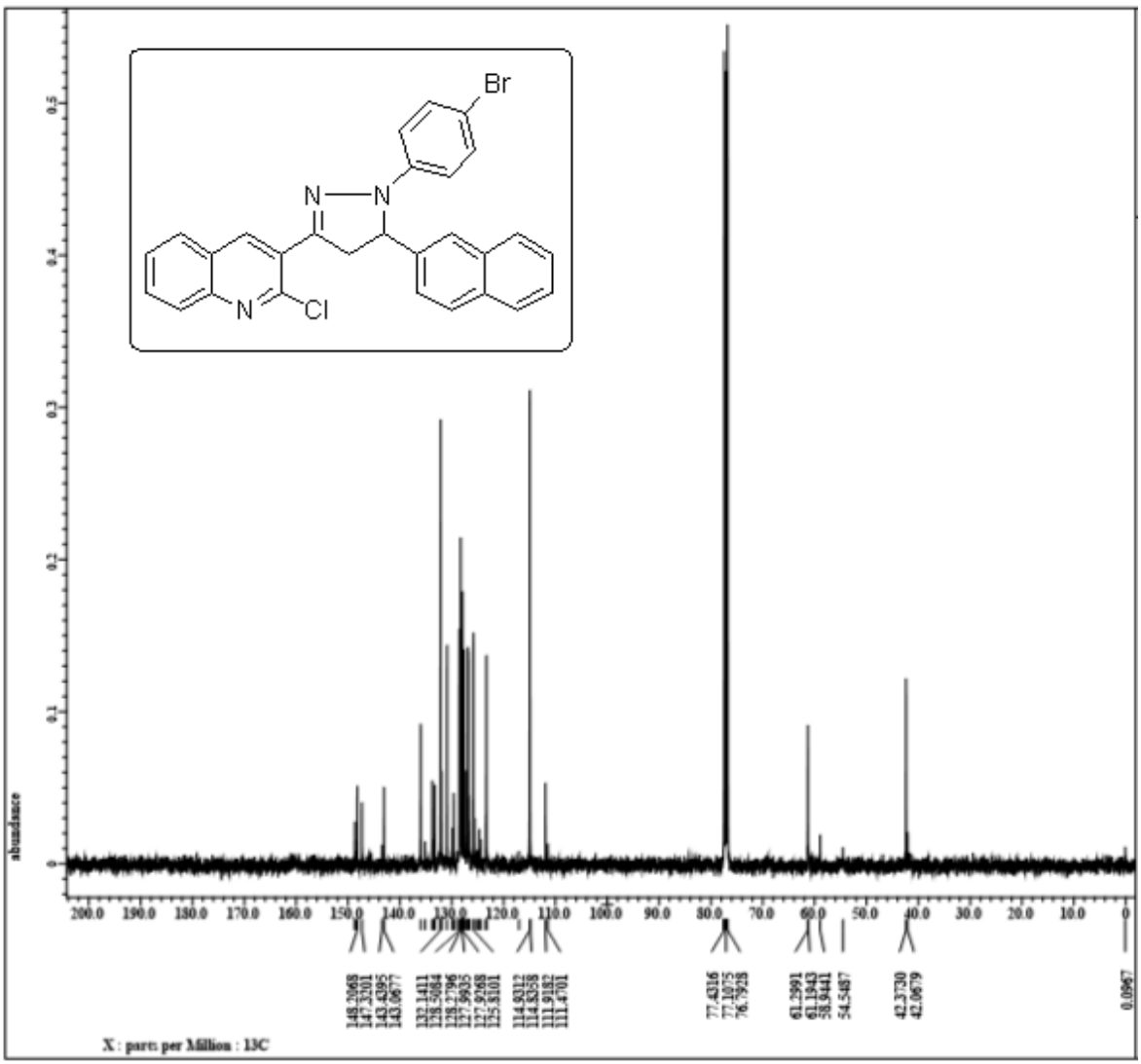

Figure 10 ^{13}C NMR spectrum of DC-1

DC-4

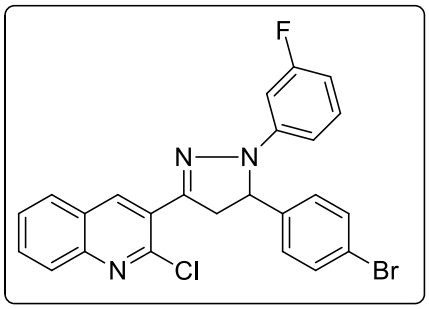

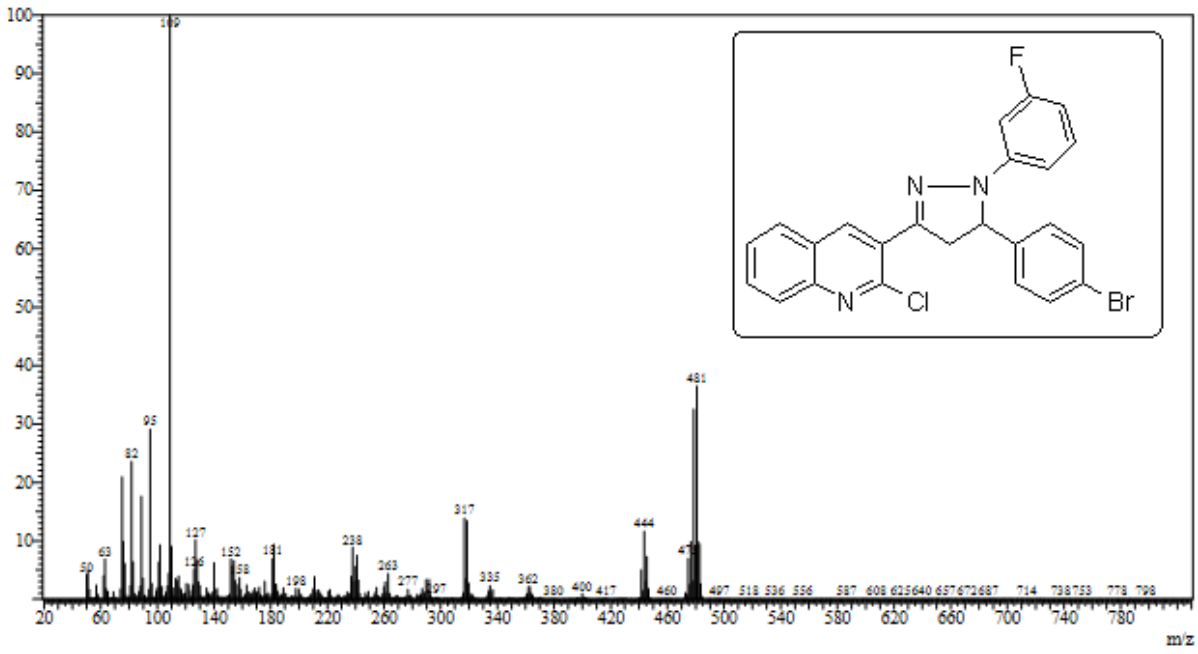

Figure 11 Mass spectrum of DC-4

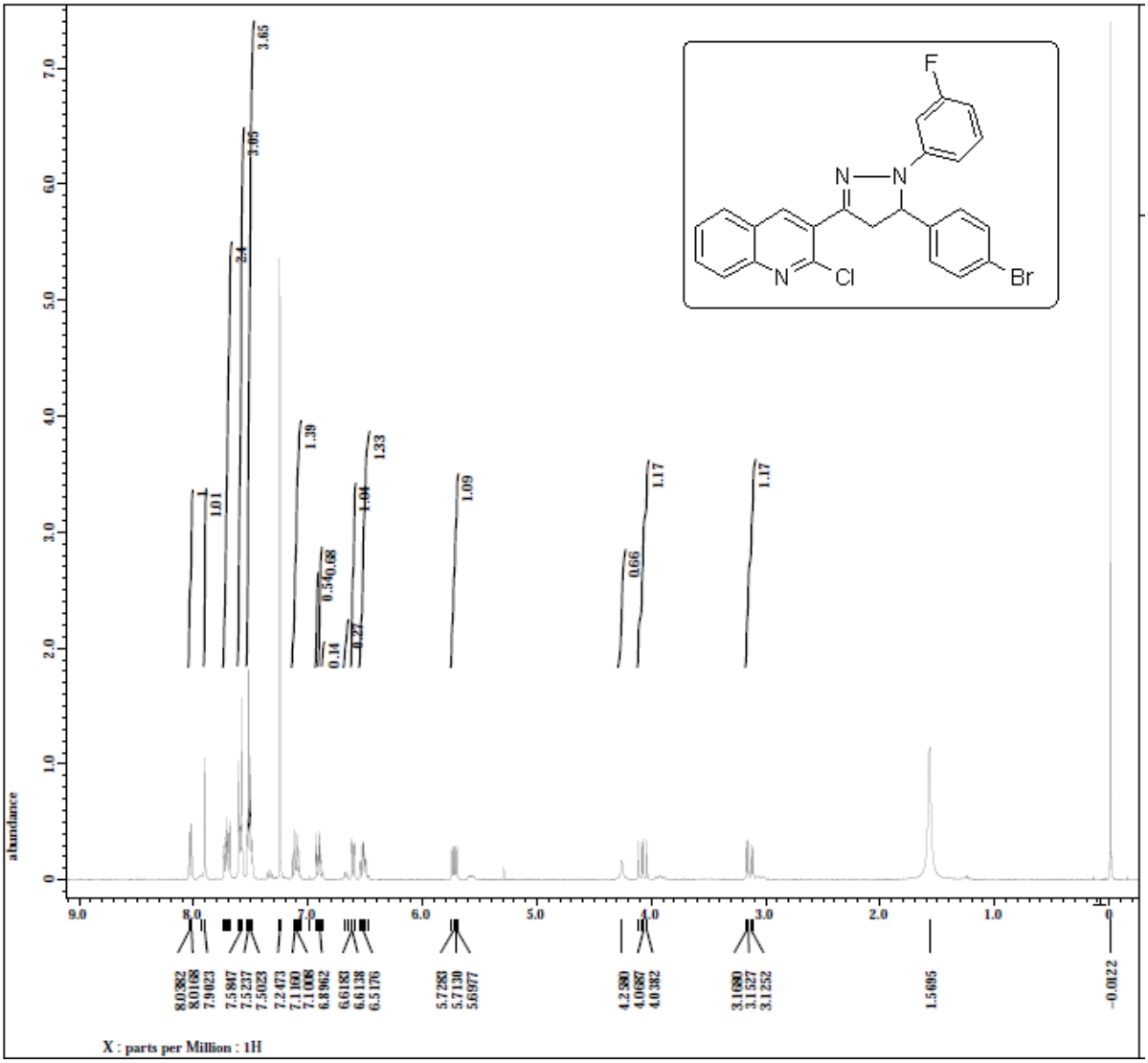

Figure12 ^{1}H-NMR of DC-4

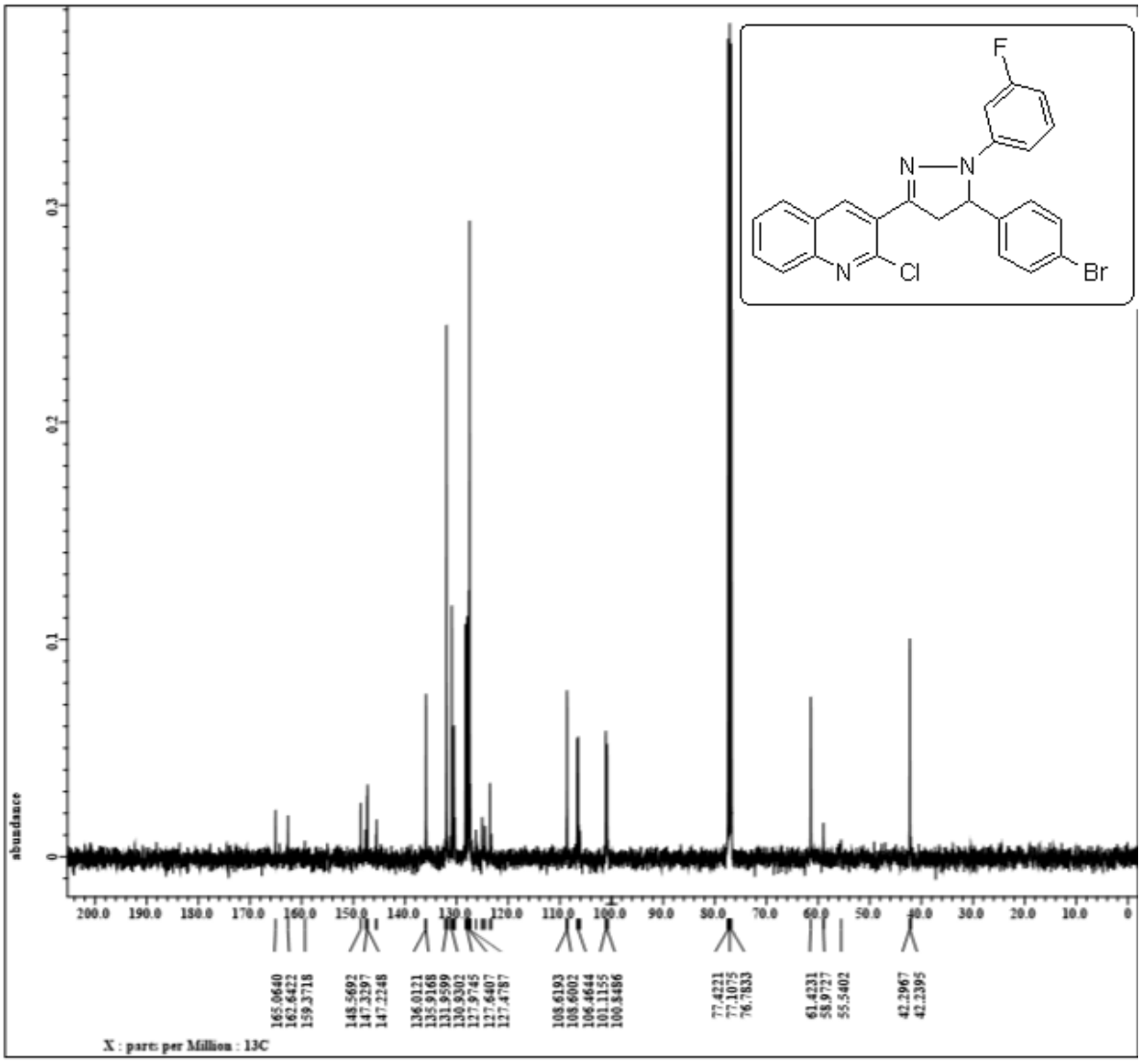

Figure13 ^{13}C NMR of DC-4

DC-5

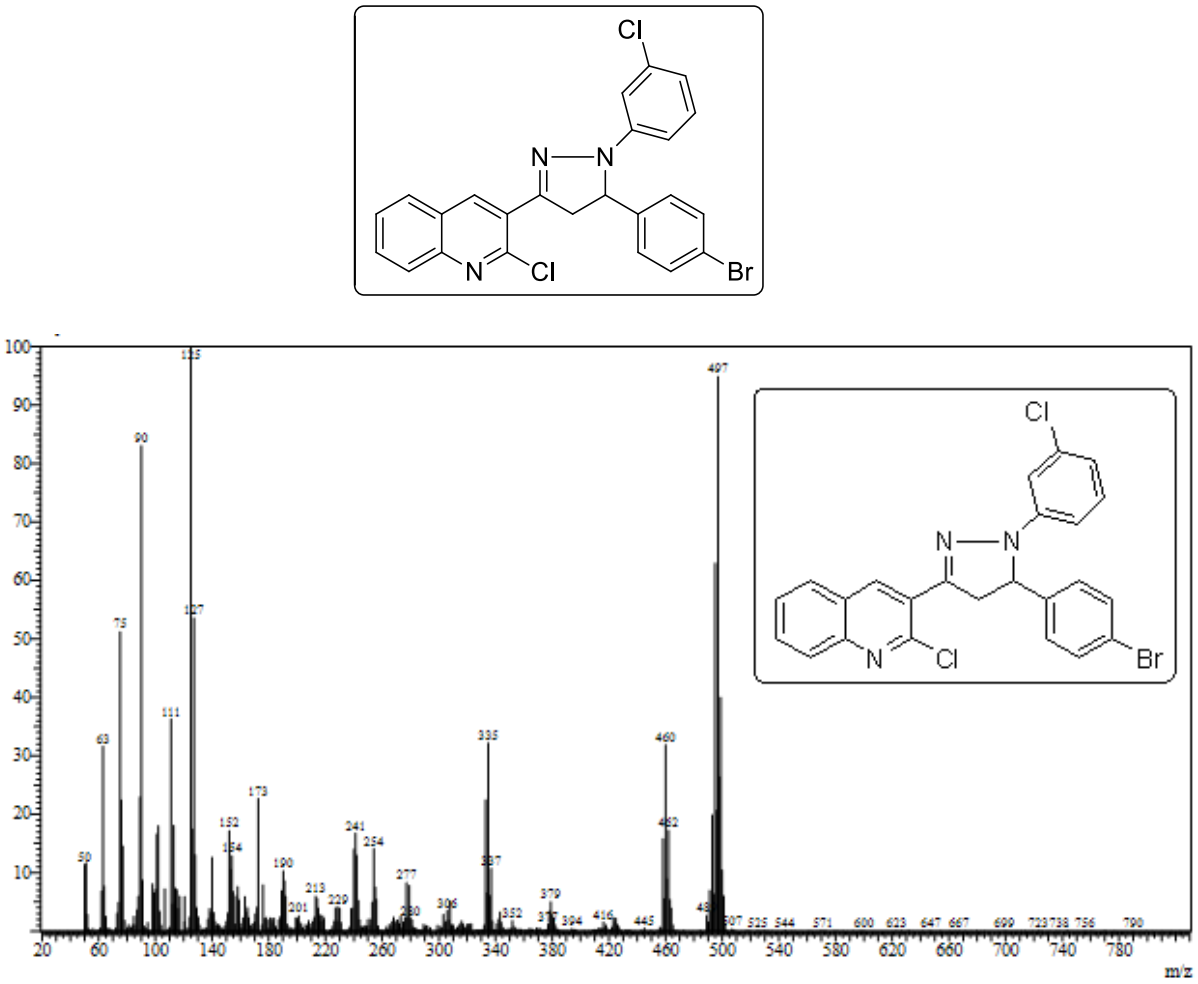

Figure 14 Mass spectrum of DC-5

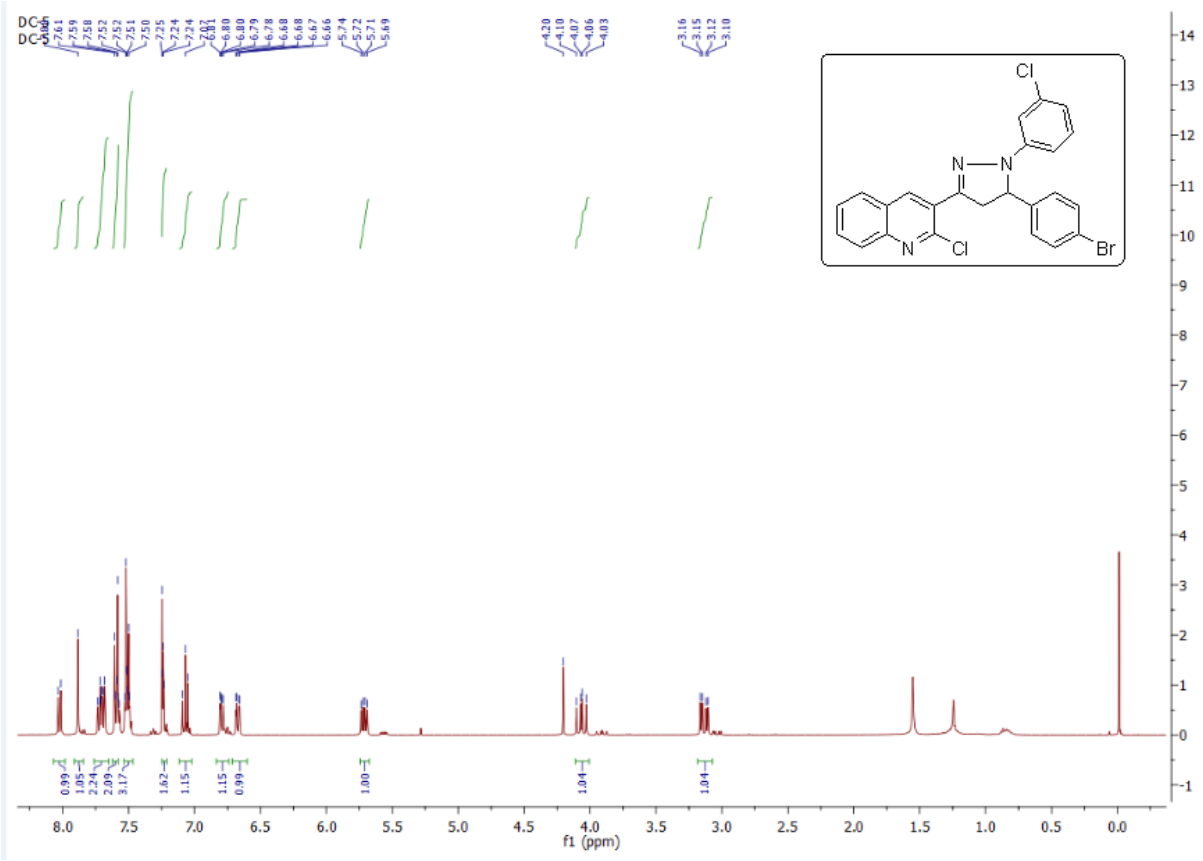

Figure 15 ^{1}H-NMR spectrum of DC-5

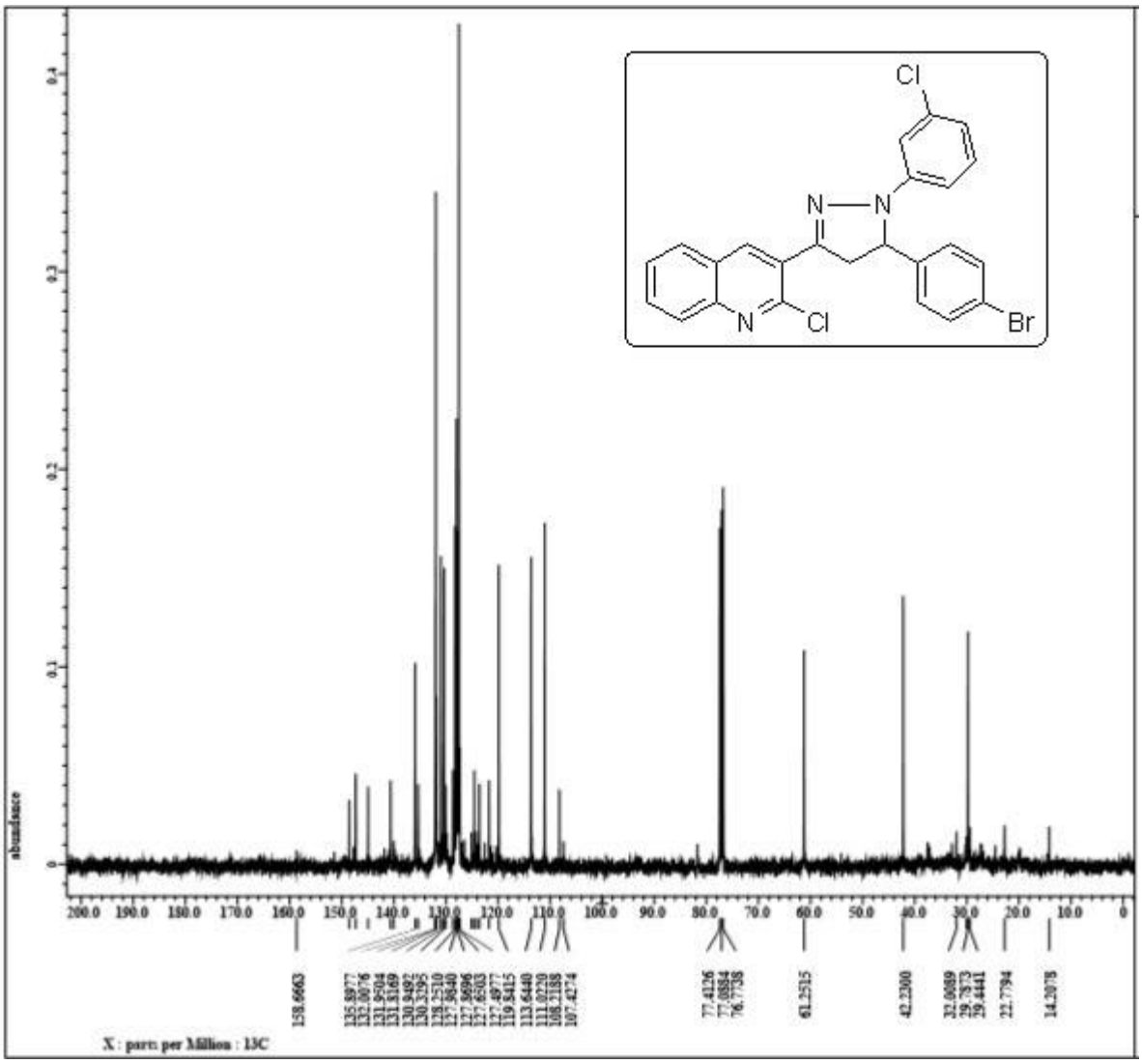

Figure 16 13C-NMR of DC-5

DC-6

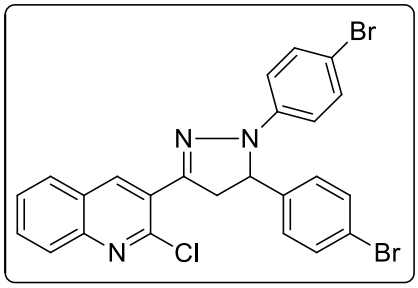

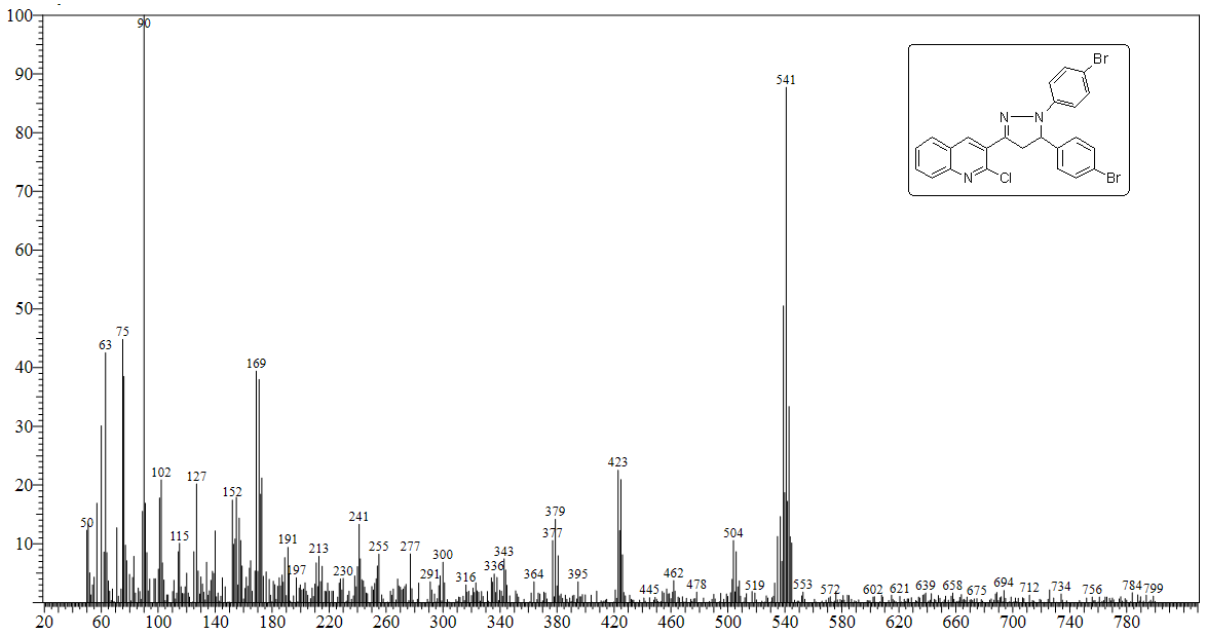

Figure 17 Mass spectrum of DC-6

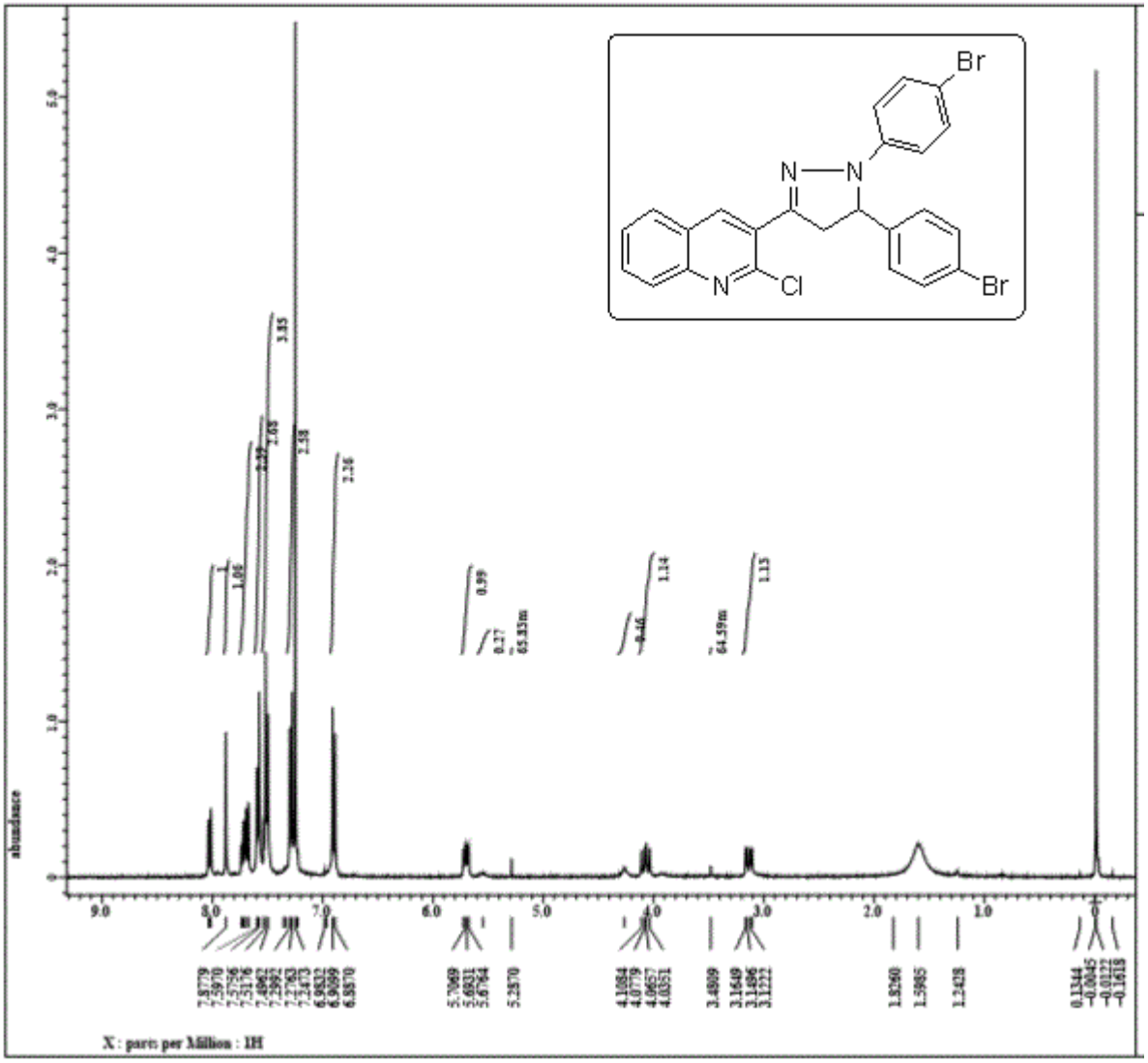

Figure 18 ^{1}H NMR of DC-6

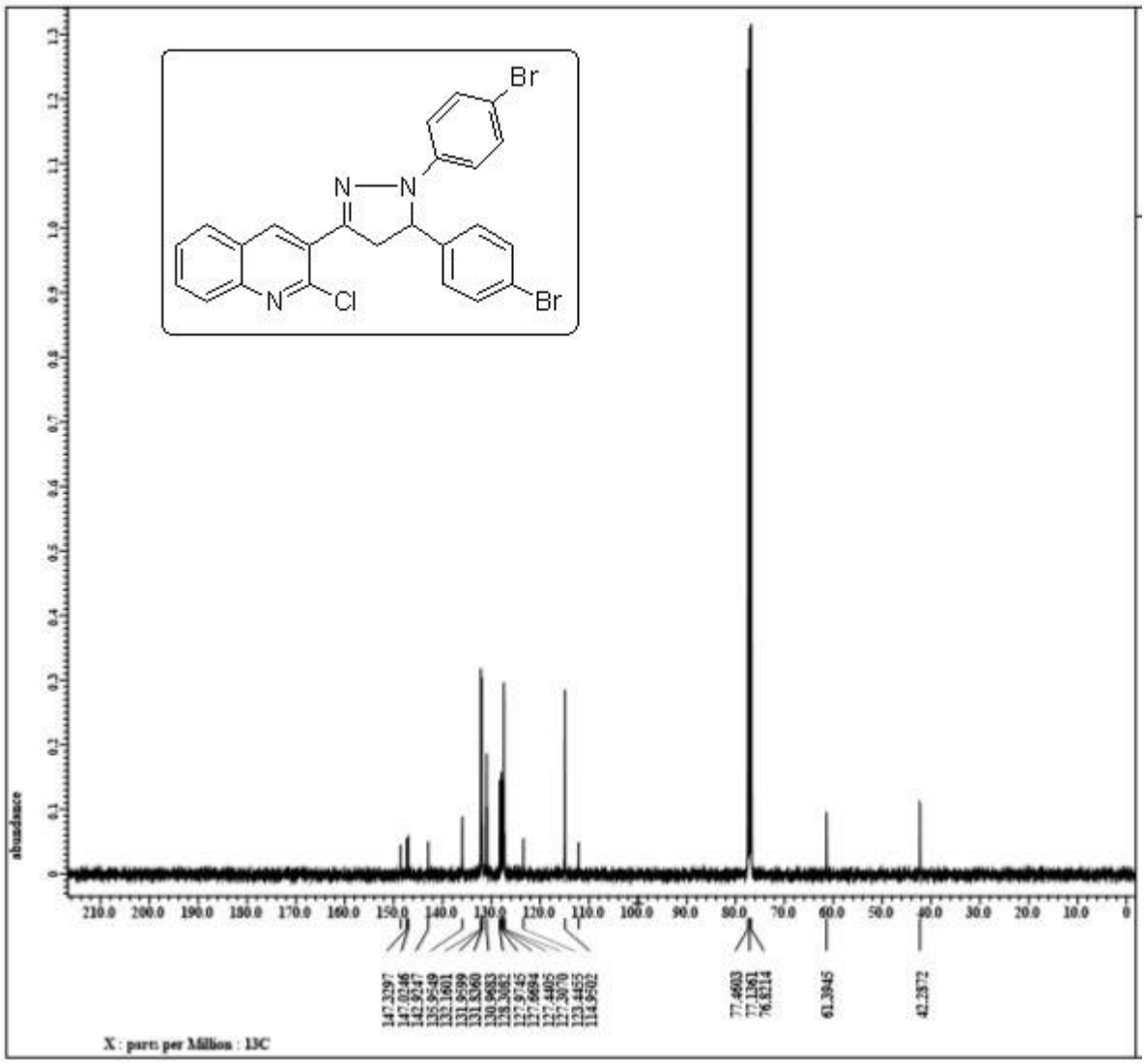

Figure 19 ^{13}C-NMR of DC-6

DC-10

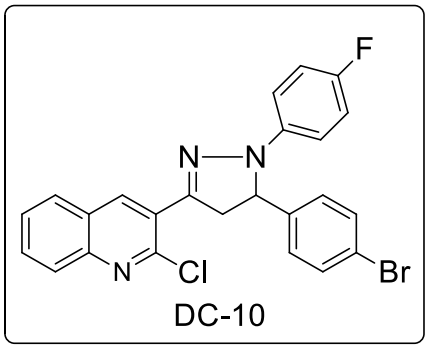

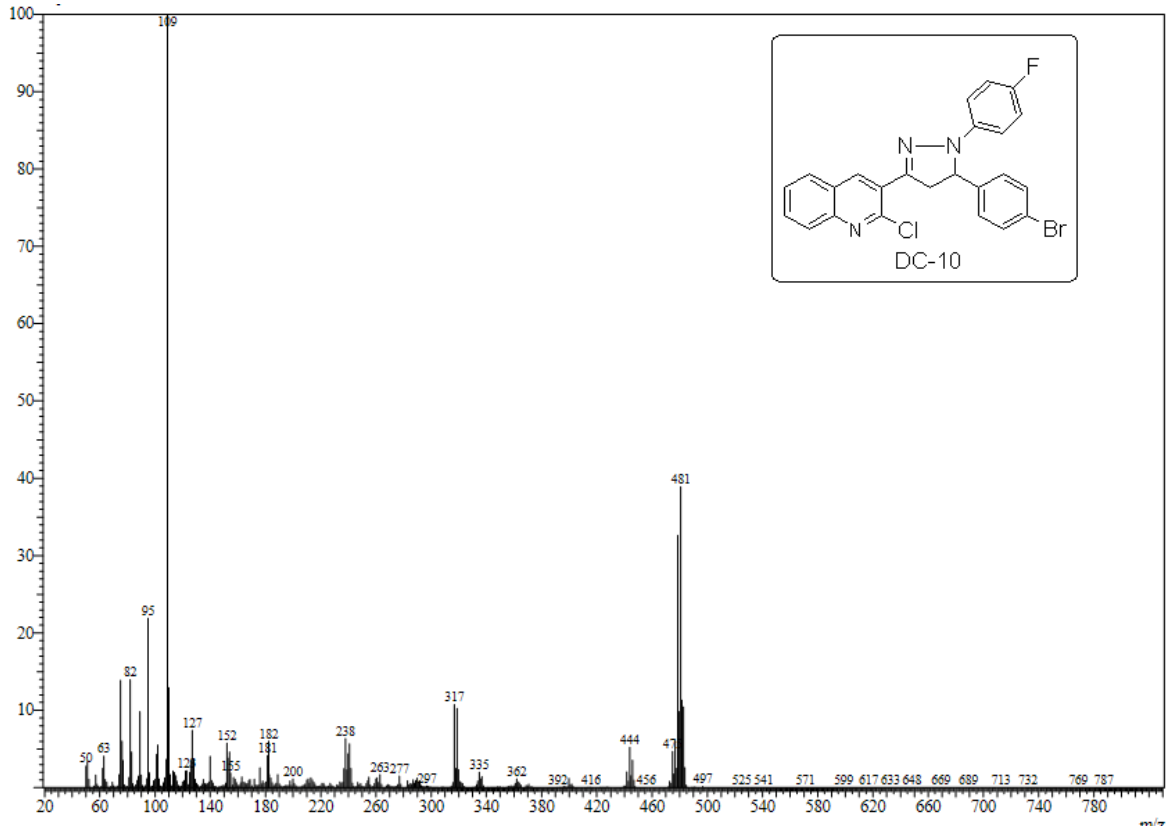

Figure 20 Mass spectrum of DC10

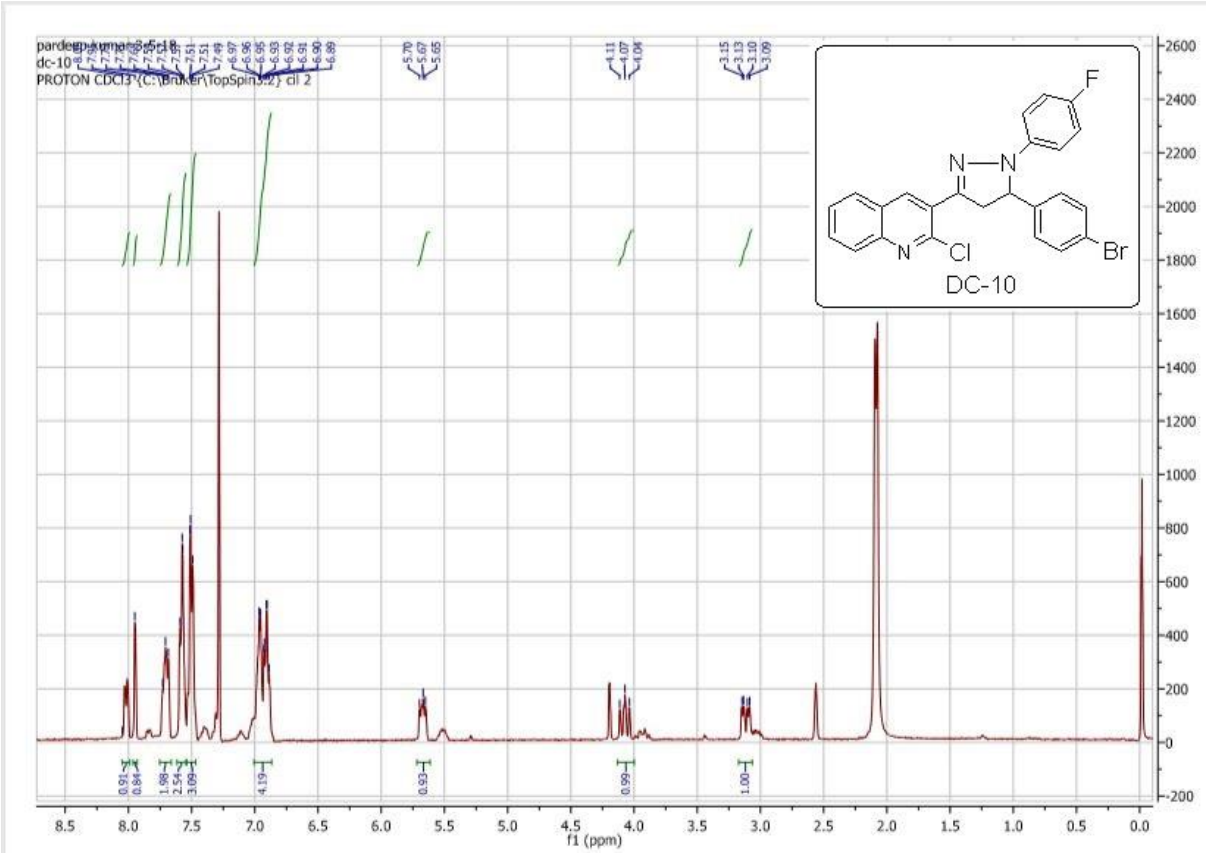

Figure 21 ^{1}H- NMR of DC10

DC-11

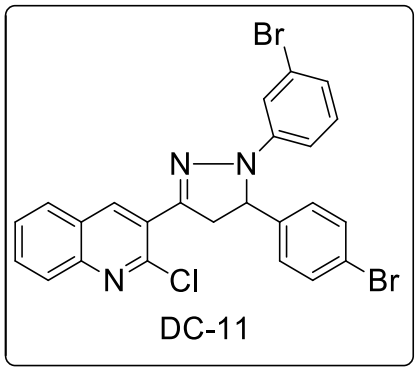

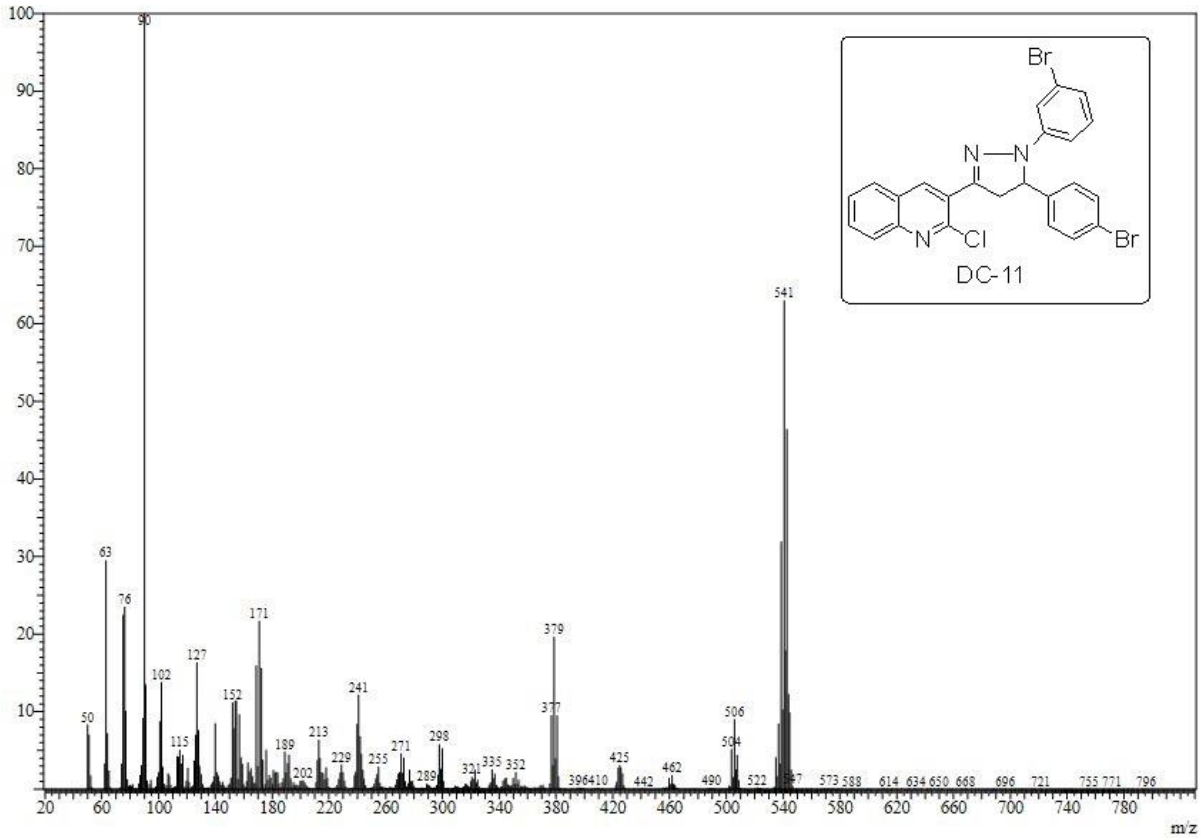

Figure 22 Mass spectrum of DC-11

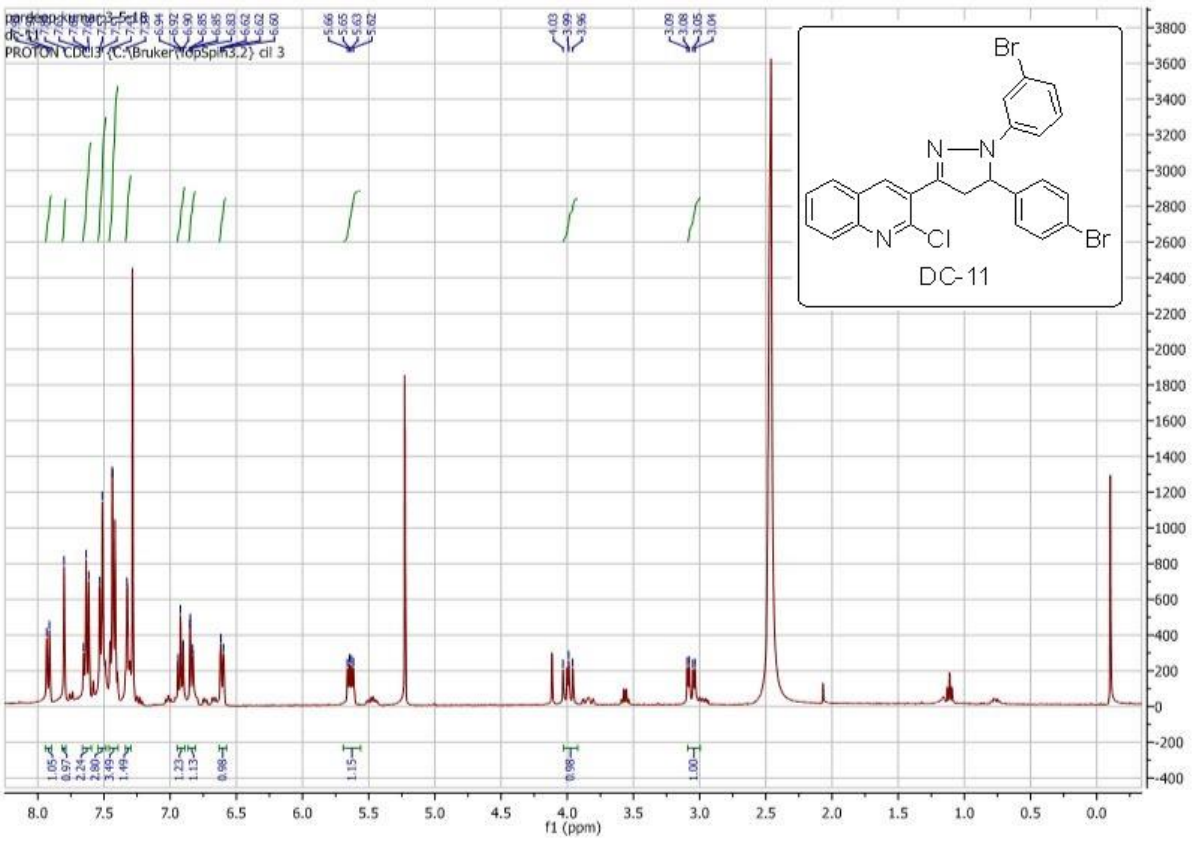

Figure 23 ^{1}H-NMR of DC-11